OXFORD

The human posterior parietal cortex: effective connectome, and its relation to function

Edmund T. Rolls[1,2,3,*], Gustavo Deco[4,5,6], Chu-Chung Huang[7,8], Jianfeng Feng[2,3]

[1]Oxford Centre for Computational Neuroscience, Oxford, United Kingdom,

[2]Department of Computer Science, University of Warwick, Coventry CV4 7AL, United Kingdom,

[3]Institute of Science and Technology for Brain Inspired Intelligence, Fudan University, Shanghai 200403, China,

[4]Computational Neuroscience Group, Department of Information and Communication Technologies, Center for Brain and Cognition, Universitat Pompeu Fabra, Roc Boronat 138, Barcelona 08018, Spain,

[5]Brain and Cognition, Pompeu Fabra University, Barcelona 08018, Spain,

[6]Institució Catalana de la Recerca i Estudis Avançats (ICREA), Universitat Pompeu Fabra, Passeig Lluís Companys 23, Barcelona 08010, Spain,

[7]Shanghai Key Laboratory of Brain Functional Genomics (Ministry of Education), School of Psychology and Cognitive Science, Institute of Brain and Education Innovation, East China Normal University, Shanghai 200602, China,

[8]Shanghai Center for Brain Science and Brain-Inspired Technology, Shanghai 200602, China

*Corresponding author: Department of Computer Science, University of Warwick, Coventry CV4 7AL, United Kingdom. Email: Edmund.Rolls@oxcns.org
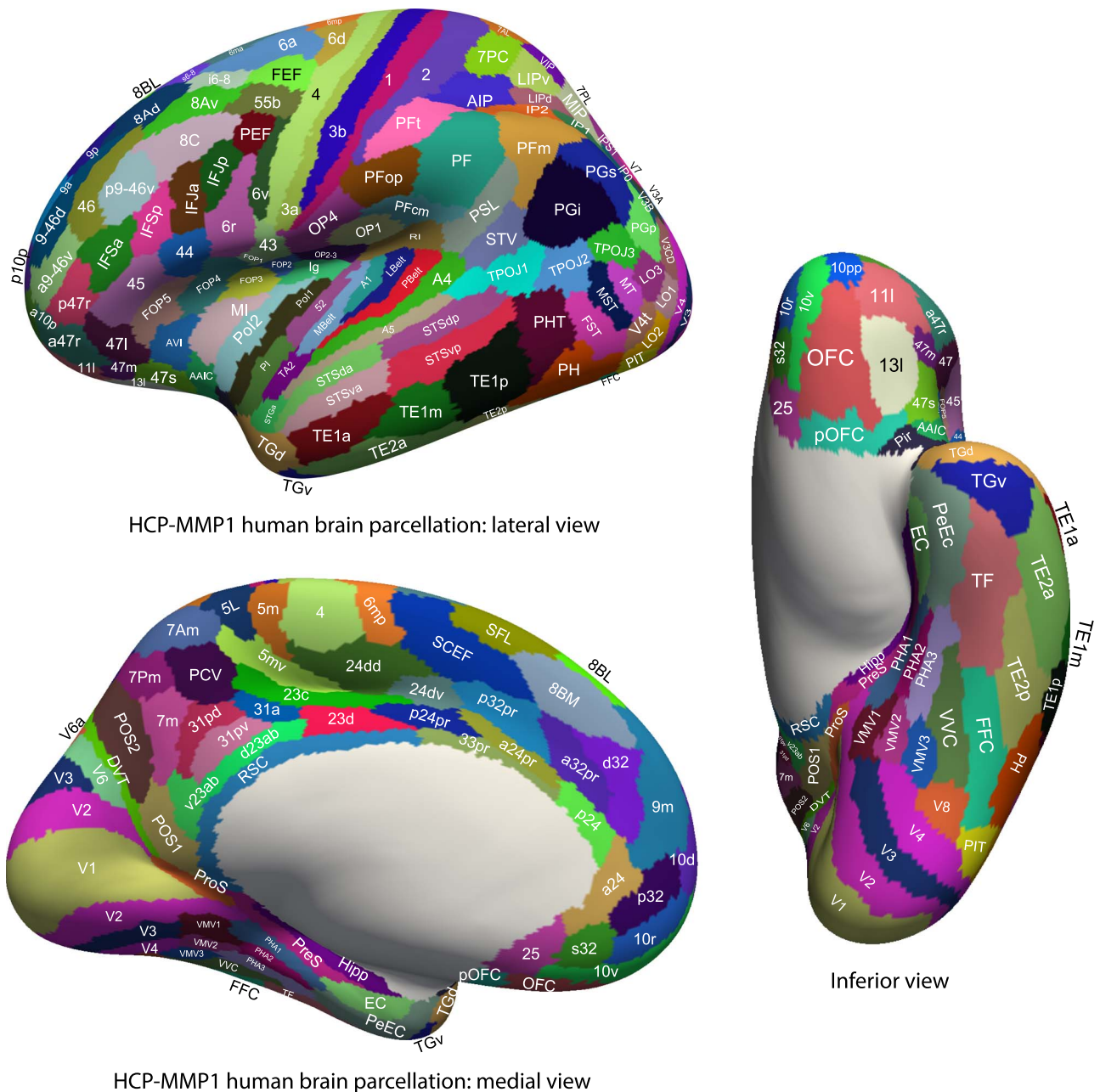
The effective connectivity between 21 regions in the human posterior parietal cortex, and 360 cortical regions was measured in 171 Human Connectome Project (HCP) participants using the HCP atlas, and complemented with functional connectivity and diffusion tractography. Intraparietal areas LIP, VIP, MIP, and AIP have connectivity from early cortical visual regions, and to visuomotor regions such as the frontal eye fields, consistent with functions in eye saccades and tracking. Five superior parietal area 7 regions receive from similar areas and from the intraparietal areas, but also receive somatosensory inputs and connect with premotor areas including area 6, consistent with functions in performing actions to reach for, grasp, and manipulate objects. In the anterior inferior parietal cortex, PFop, PFt, and PFcm are mainly somatosensory, and PF in addition receives visuo-motor and visual object information, and is implicated in multimodal shape and body image representations. In the posterior inferior parietal cortex, PFm and PGs combine visuo-motor, visual object, and reward input and connect with the hippocampal system. PGi in addition provides a route to motion-related superior temporal sulcus regions involved in social interactions. PGp has connectivity with intraparietal regions involved in coordinate transforms and may be involved in idiothetic update of hippocampal visual scene representations.

Key words: parietal cortex; memory; navigation; visuo-motor coordinate transforms; spatial view; touch.

Introduction

The human posterior parietal cortex (Critchley 1953; Berlucchi and Vallar 2018) is usually divided into superior and inferior parts (Fig. 1 and Fig. S1–5). The superior part contains cortical regions in area 7 and the intraparietal sulcus that in macaques are involved in visuomotor control for eye movements and reaching and hand movements in space (Andersen and Cui 2009; Gamberini et al. 2020; Passarelli et al. 2021). Intraparietal sulcus regions in humans are implicated in the fine eye movement control required for reading, and in numerosity (the ability to rapidly extract the number of items from a visual scene) (Lasne et al. 2019). In macaques, the dorsal visual stream is organized into 2 main routes. In a dorsomedial "reach-to-grasp" network, visual information from V1 involves parietal areas of the superior parietal lobule (SPL) (including V6, V6A, PEc, and MIP) and reaches the dorsal premotor areas (PMd/F2) (Gamberini et al. 2020; Passarelli et al. 2021). A "lateral grasping" network in macaques involves areas of the inferior parietal lobule and reaches the ventral premotor area PMv (Gamberini et al. 2020; Passarelli et al. 2021).

In humans, the greatly developed inferior parietal lobule contains posteriorly PG areas (shown in Fig. 1) found in BA39 in the angular gyrus, which are implicated in memory and semantic processing, with damage on the left related to dyslexia and agraphia and on the right to body image (Caspers et al. 2008; Davis et al. 2018). The angular gyrus is part of the "default mode network," which is active in the resting state, and is deactivated in many tasks (Raichle et al. 2001; Buckner et al. 2008; Andrews-Hanna et al. 2014). However, these are typically tasks in which there is an external stimulus. If memory is used to initiate a task, then key regions in the default mode network, including prefrontal cortical short-term memory areas, become active (Passingham 2021), and so do the connected posterior parietal cortical areas (Papagno 2018). To clarify, the use of memory to initiate tasks may be a key to understanding the prefrontal cortex (and also its connectivity with parietal areas), so that "memory-guided action" may be a useful description for functions of the prefrontal cortex, rather than ascriptions such as "voluntary action" (Passingham 2021). Correspondingly, the default mode network might

HCP-MMP1 human brain parcellation: lateral view

HCP-MMP1 human brain parcellation: medial view

Inferior view

Fig. 1. Anatomical regions of the human posterior parietal cortex. Regions of the posterior parietal cortex as defined in the HCP-MMP atlas (Glasser, Coalson, et al. 2016a), and in its extended version HCPex (Huang et al. 2022). The regions are shown on images of the human brain with the sulci expanded sufficiently to allow the regions within the sulci to be shown. Abbreviations are provided in Table S1. The regions are as follows. Superior parietal area 7: 7AL, 7Am, 7PC, 7PL, 7Pm. Intraparietal sulcus regions: AIP, LIPd, LIPv, MIP, VIP, IP0, IP1, IP2. Inferior parietal: PFcm, PGop, PFt, PF, PFm; PGi, PGs, PGp. For comparison, a version of this diagram without the sulci expanded is provided in Fig. S1–5.

be operationally understood as the memory-guided network. The angular gyrus has also been implicated in some aspects of spatial attention and neglect (Vallar and Calzolari 2018). The anterior part of the angular gyrus has resting state functional connectivity with ventral premotor areas and ventrolateral prefrontal cortex; and the posterior part of the angular gyrus (PGp) has functional connectivity with ventromedial prefrontal cortex, the posterior cingulate, and the hippocampus (Uddin et al. 2010; Baker et al. 2018).

The human inferior parietal lobule contains anteriorly BA40 in the supramarginal gyrus which can be divided into PF, PFcm, PFm, PFop, and PFt (Caspers et al. 2008;

Baker et al. 2018; Caspers and Zilles 2018) (Fig. 1), and in macaques these PF areas contain neurons that respond to limb movement or the sight of movement, or both if they are "mirror neurons" (Rizzolatti and Rozzi 2018). In macaques, anterior PF regions had neurons related to mouth movements, posterior PF regions had activity related to hand actions, and PG regions had neurons related to arm and eye movements (Rizzolatti and Rozzi 2018). In humans, the PF areas on the left are related to phonology (Davis et al. 2018).

The human parietal cortex has connectivity with the hippocampal system involved in memory and spatial navigation, with the connectivity involving in

part the posterior cingulate/retrosplenial (RSC) cortex (Uddin et al. 2010; Kravitz et al. 2011; Rolls, Wirth, et al. 2022). The relative roles of the hippocampal system and the parietal cortex in navigation are of considerable interest, going beyond the concept that the hippocampus is the main brain system involved in navigation. Lesions to the human neocortex can produce topographical agnosia and inability to navigate (Barton 2011; Kolb and Whishaw 2015), and the retrosplenial cortex (RSC) is implicated in navigation (Byrne et al. 2007; Epstein 2008; Vann et al. 2009; Alexander and Nitz 2015; Vedder et al. 2017). In more detail, lesions restricted to the hippocampus in humans result in only slight navigation impairments in familiar environments, but rather strongly impair learning or imagining new trajectories (Teng and Squire 1999; Spiers and Maguire 2006; Bohbot and Corkin 2007; Clark and Maguire 2016; Maguire et al. 2016). In contrast, lesions in regions such as the parietal cortex or the retrosplenial cortex produce strong topographical disorientation in both familiar and new environments (Habib and Sirigu 1987; Takahashi et al. 1997; Aguirre and D'Esposito 1999; Maguire 2001; Kim et al. 2015). This suggests that the core navigation processes (which may include transformations from allocentric representations to egocentric motor commands) are performed independently by neocortical areas outside the hippocampus, which may utilize hippocampal information related to recent memories (Miller et al. 2013; Ekstrom et al. 2014). That would suggest that the role of the hippocampal system in navigation is related at least in part to its functions in object-location episodic memory and recall (Rolls 2021a, 2021c). This emphasizes the importance of better understanding of the connectivity and functions of the human parietal cortex, and its connectivity with the posterior cingulate/RSC, for understanding of brain navigation systems in humans.

Given the great development and heterogeneity of functions of different parts of the human posterior parietal cortex, and the importance for understanding brain computations of evidence about the connectivity of different brain regions (Rolls 2021c), the aim of the present investigation was to advance understanding of the connections and connectivity of the human posterior parietal cortex. To do this, we measured with Human Connectome Project (HCP) data (Glasser, Smith, et al. 2016b) the direct connections between brain regions using diffusion tractography; the functional connectivity between brain regions using the correlation between the BOLD signals in resting state functional magnetic resonance (fMRI), which provides evidence about the strength of interactions; and the effective connectivity which provides evidence about the strength and direction of the causal connectivity between pairs of hundreds of brain regions with a new Hopf algorithm (Rolls, Deco, et al. 2022b, 2022c, 2022d). These measures were made between the 360 cortical regions in the HCP-multimodal parcellation atlas (HCP-MMP) (Glasser,

Coalson, et al. 2016a). The HCP-MMP atlas provides the most detailed parcellation of the human cortical areas that we know, in that its 360 regions are defined using a combination of structural measures (cortical thickness and cortical myelin content), functional connectivity, and task-related fMRI (Glasser, Coalson, et al. 2016a). This parcellation is the parcellation of choice for the cerebral cortex because it is based on multimodal information (Glasser, Coalson, et al. 2016a) with the definitions and boundaries set out in their Glasser_2016_SuppNeuroanatomy.pdf, and it is being used as the basis for many new investigations of brain function and connectivity, which can all be cast in the same framework (Colclough et al. 2017; Van Essen and Glasser 2018; Sulpizio et al. 2020; Yokoyama et al. 2021; Rolls, Deco, et al. 2022b, 2022c, 2022d). This approach provides better categorization of cortical areas than does for example functional connectivity alone (Power et al. 2011). A summary of the boundaries, tractography, functional connectivity, and task-related activations of lateral parietal areas using the HCP-MMP atlas is available elsewhere (Glasser, Coalson, et al. 2016a; Baker et al. 2018), but the effective connectivity, tractography, and functional connectivity analyses described here are new, and further are presented in quantitative form using connectivity matrices for all 360 cortical region.

Strengths of this investigation are that it utilized this HCP-MMP1 atlas; HCP data from the same set of 171 participants imaged at 7T (Glasser, Smith, et al. 2016b) in whom we could calculate the connections, functional connectivity, and effective connectivity; and that it utilized a method for effective connectivity measurement between all 360 cortical regions investigated here.

Methods
Participants and data acquisition

Multiband 7 T resting-state fMRI (rs-fMRI) images of 184 individuals were obtained from the publicly available S1200 release (last updated: April 2018) of the HCP (Van Essen et al. 2013). Individual written informed content was obtained from each participant, and the scanning protocol was approved by the Institutional Review Board of Washington University in St. Louis, MO, USA (IRB #201204036).

Multimodal imaging was performed in a Siemens Magnetom 7 T housed at the Center for Magnetic Resonance (CMRR) at the University of Minnesota in Minneapolis. For each participant, a total of 4 sessions of rs-fMRI were acquired, with oblique axial acquisitions alternated between phase encoding in a posterior-to-anterior (PA) direction in sessions 1 and 3, and an anterior-to-posterior (AP) phase encoding direction in sessions 2 and 4. Specifically, each rs-fMRI session was acquired using a multiband gradient-echo EPI imaging sequence. The following parameters were used: TR $= 1,000$ ms, TE $= 22.2$ ms, flip angle $= 45°$, field of view $= 208 \times 208$, matrix $= 130 \times 130$, 85 slices, voxel

size $= 1.6 \times 1.6 \times 1.6$ mm^3, multiband factor $= 5$. The total scanning time for the rs-fMRI protocol was ~16 min with 900 volumes. Further details of the 7T rs-fMRI acquisition protocols are given in the HCP reference manual (https://humanconnectome.org/storage/app/media/documentation/s1200/HCP_S1200_Release_Reference_Manual.pdf).

The current investigation was designed to complement investigations of effective and functional connectivity and diffusion tractography of the hippocampus (Huang et al. 2021; Ma et al. 2022; Rolls, Deco, et al. 2022d) and posterior cingulate cortex (Rolls, Wirth, et al. 2022), and so the same 171 participants with data for the first session of rs-fMRI at 7T were used for the analyses described here (age 22–36 years, 66 males).

Data preprocessing

The preprocessing was performed by the HCP as described in Glasser et al. (2013), based on the updated 7T data pipeline (v3.21.0, https://github.com/Washington-University/HCPpipelines), including gradient distortion correction, head motion correction, image distortion correction, spatial transformation to the Montreal Neurological Institute space using one step spline resampling from the original functional images followed by intensity normalization. In addition, the HCP took an approach using ICA (FSL's MELODIC) combined with a more automated component classifier referred to as FIX (FMRIB's ICA-based X-noisifier) to remove non-neural spatiotemporal artifact (Smith et al. 2013; Griffanti et al. 2014; Salimi-Khorshidi et al. 2014). This step also used 24 confound timeseries derived from the motion estimation (6 rigid-body parameter timeseries, their backwards-looking temporal derivatives, plus all 12 resulting regressors squared (Satterthwaite et al. 2013) to minimize noise in the data. The preprocessing performed by the HCP also included boundary-based registration between EPI and T1w images, and brain masking based on FreeSurfer segmentation. The "minimally preprocessed" rsfMRI data provided by the HCP 1200 release (rfMRI*hp2000_clean.dtseries) were used in this investigation. The preprocessed data are in the HCP grayordinates standard space and are made available in a surface-based Connectivity Informatics Technology Initiative (CIFTI) file for each participant. With the MATLAB script (cifti toolbox: https://github.com/Washington-University/cifti-matlab), we extracted and averaged the cleaned timeseries of all the grayordinates in each region of the HCP-MMP 1.0 atlas (Glasser, Coalson, et al. 2016a), which is a group-based parcellation defined in the HCP gray ordinate standard space having 180 cortical regions per hemisphere, and is a surface-based atlas provided in CIFTI format. The timeseries were detrended, and temporally filtered with a second order Butterworth filter set to 0.008–0.08 Hz.

Brain atlas and region selection

To construct the effective connectivity for the regions of interest in this investigation with other parts of the human brain, we utilized the 7T resting state fMRI data the HCP, and parcellated this with the surface based HCP-MMP1 atlas which has 360 cortical regions (Glasser, Coalson, et al. 2016a). We were able to use the same 171 participants for whom we also had performed diffusion tractography, as described in detail (Huang et al. 2021). All 20 parietal regions listed in Table S1 as in the Superior and Inferior Parietal divisions by Glasser, Coalson, et al. (2016a) were included, and to these was added PFcm, as that is part of the parietal cortex. This analysis focused on the posterior parietal cortex, and did not include the somatosensory areas 1–3 and 5. The brain regions are shown in Fig. 1 and Fig. S1, and a list of the cortical regions in this atlas is provided in Table S1 in the reordered form used in the extended volumetric HCPex atlas (Huang et al. 2022). The timeseries for the 4 sessions for each participant were extracted for each region in the surface-based atlas using the HCP protocol and software (Glasser, Coalson, et al. 2016a), and the functional connectivity and effective connectivity were measured using all 4 timeseries for each of the 171 participants as described below. The connectivity of some medial parietal regions such as 7m and precuneus visual area (PCV) are included in a previous investigation (Rolls, Wirth, et al. 2022) as they are included in the Posterior Cingulate division of the HCP-MMP1 atlas (Glasser, Coalson, et al. 2016a) as shown in Table S1.

Measurement of effective connectivity

Effective connectivity measures the effect of one brain region on another, and utilizes differences detected at different times in the signals in each connected pair of brain regions to infer effects of one brain region on another. One such approach is dynamic causal modeling, but it applies most easily to activation studies, and is typically limited to measuring the effective connectivity between just a few brain areas (Friston 2009; Valdes-Sosa et al. 2011; Bajaj et al. 2016), though there have been moves to extend it to resting state studies and more brain areas (Frassle et al. 2017; Razi et al. 2017). The method used here (see Rolls, Deco, et al. 2022b, 2022c, 2022d) was developed from a Hopf algorithm to enable measurement of effective connectivity between many brain areas, described by Deco et al. (2019). A principle is that the functional connectivity is measured at time t and time $t +$ tau, where tau is typically 2 s to take into account the time within which a change in the BOLD signal can occur, and that tau should be short to capture causality, and then the effective connectivity model is trained by error correction until it can generate the functional connectivity matrices at time t and time t + tau. Further details of the algorithm, and the development that enabled it to measure the effective connectivity in each direction, are described next and in more detail in the Supplementary Material.

To infer the effective connectivity, we use a whole-brain model that allows us to simulate the BOLD activity across all brain regions and time. We use the so-called Hopf computational model, which integrates the dynam-

ics of Stuart-Landau oscillators, expressing the activity of each brain region, by the underlying anatomical connectivity (Deco, Kringelbach, et al. 2017b). As mentioned above, we include in the model 360 cortical brain areas (Huang et al. 2022). The local dynamics of each brain area (node) is given by Stuart-Landau oscillators which express the normal form of a supercritical Hopf bifurcation, describing the transition from noisy to oscillatory dynamics (Kuznetsov 2013). During the last years, numerous studies were able to show how the Hopf whole-brain model successfully simulates empirical electrophysiology (Freyer et al. 2011; Freyer et al. 2012), MEG (Deco, Cabral, et al. 2017a), and fMRI (Kringelbach et al. 2015; Deco, Kringelbach, et al. 2017b; Kringelbach and Deco 2020).

The Hopf whole-brain model can be expressed mathematically as follows:

$$\frac{\mathrm{d}x_i}{\mathrm{d}t} = \overbrace{\left[a_i - x_i^2 - y_i^2\right]x_i - \omega_i y_i}^{\text{Local Dynamics}}$$

$$+ \overbrace{G\sum_{j=1}^{N} C_{ij}\left(x_j - x_i\right)}^{\text{Coupling}} + \overbrace{\beta\eta_i(t)}^{\text{Gaussian Noise}} \qquad (1)$$

$$\frac{\mathrm{d}y_i}{\mathrm{d}t} = \left[a_i - x_i^2 - y_i^2\right]y_i + \omega_i x_i + G\sum_{j=1}^{N} C_{ij}\left(y_j - y_i\right) + \beta\eta_i(t) \quad (2)$$

Equations (1) and (2) describe the coupling of Stuart-Landau oscillators through an effective connectivity matrix C. The $x_i(t)$ term represents the simulated BOLD signal data of brain area i. The values of $y_i(t)$ are relevant to the dynamics of the system but are not part of the information read out from the system. In these equations, $\eta_i(t)$ provides additive Gaussian noise with standard deviation β. The Stuart-Landau oscillators for each brain area i express a Hopf normal form that has a supercritical bifurcation at $a_i = 0$, so that if $a_i > 0$ the system has a stable limit cycle with frequency $f_i = \omega_i/2\pi$ (where ω_i is the angular velocity); and when $a_i < 0$ the system has a stable fixed point representing a low activity noisy state. The intrinsic frequency f_i of each Stuart-Landau oscillator corresponding to a brain area is in the 0.008–0.08 Hz band ($i = 1, \ldots, 360$). The intrinsic frequencies are fitted from the data, as given by the averaged peak frequency of the narrowband BOLD signals of each brain region. The coupling term representing the input received in node i from every other node j, is weighted by the corresponding effective connectivity C_{ij}. The coupling is the canonical diffusive coupling, which approximates the simplest (linear) part of a general coupling function. G denotes the global coupling weight, scaling equally the total input received in each brain area. While the oscillators are weakly coupled, the periodic orbit of the uncoupled oscillators is preserved. Details of the algorithm, how it was applied, and that use of the anatomical connection matrix was not in practice important for these analyses, are provided in the Supplementary Material.

The effective connectivity matrix is derived by optimizing the conductivity of each existing anatomical connection as specified by the Structural Connectivity matrix (measured with tractography (Huang et al. 2021)) in order to fit the empirical functional connectivity (FC) pairs and the lagged FC$^{\text{tau}}$ pairs. By this, we are able to infer a non-symmetric Effective Connectivity matrix (see Gilson et al. (2016)). Note that FC$^{\text{tau}}$, i.e. the lagged functional connectivity between pairs, lagged at tau s, breaks the symmetry and thus is fundamental for our purpose. Specifically, we compute the distance between the model FC simulated from the current estimate of the effective connectivity and the empirical data FC$^{\text{emp}}$, as well as the simulated model FC$^{\text{tau}}$ and empirical data FC$^{\text{tau\_emp}}$ and adjust each effective connection (entry in the effective connectivity matrix) separately with a gradient-descent approach. The model is run repeatedly with the updated effective connectivity until the fit converges towards a stable value.

We start with the anatomical connectivity obtained with probabilistic tractography from dMRI (or from an initial zero C matrix as described in the Supplementary Material) and use the following procedure to update each entry C_{ij} in the effective connectivity matrix

$$C_{ij} = C_{ij} + \varepsilon\left(FC_{ij}^{\text{emp}} - FC_{ij} + FC_{ij}^{\text{tau\_emp}} - FC_{ij}^{\text{tau}}\right) \qquad (3)$$

where ϵ is a learning rate constant, and i and j are the nodes. When updating each connection if the initial matrix is a dMRI structural connection matrix (see Supplementary Material), the corresponding link to the same brain regions in the opposite hemisphere is also updated, as contralateral connections are not revealed well by dMRI. The convergence of the algorithm is illustrated by Rolls, Deco, et al. (2022d), and the utility of the algorithm was validated as described below.

For the implementation, we set tau to be 2 s, selecting the appropriate number of TRs to achieve this. The maximum effective connectivity was set to a value of 0.2, and was found between contralateral V1 and V2.

Effective connectome

Whole-brain effective connectivity (EC) analysis was performed between the 21 regions of the posterior parietal cortex described above (see Fig. 1 and Fig. S1) and the 360 regions defined in the surface-based HCP-MMP1 atlas (Glasser, Coalson, et al. 2016a) in their reordered form provided in Table S1, described in the Supplementary Material, and used in the volumetric extended HCPex atlas (Huang et al. 2022). This EC was computed for all 171 participants. The effective connectivity algorithm was run until it had reached the maximal value for the correspondence between the simulated and empirical functional connectivity matrices at time t and t + tau (see Supplementary Material).

The effective connectivity calculated between the 360 cortical areas was checked and validated in a number of ways. First, in all cases the 360×360 effective connectivity matrix could be used to generate by simulation 360×360 functional connectivity matrices for time t and time $t + $ tau that were correlated 0.8 or more with the empirically measured functional connectivity matrices at time t and time $t + $ tau using fMRI. Second, the effective connectivity matrices were robust with respect to the number of participants, in that when the 171 participants were separated into two groups of 86, the correlation between the effective connectivities measured for each group independently was 0.98. Third, the effective connectivities for early visual areas V1, V2, V3, and V4 were compared with the known connections for forward and backward connections involving these areas in macaques (Markov et al. 2014), and the human effective connectivity was consistent with the connections in this hierarchically organized system in macaques, with these results shown in Rolls, Deco, et al. (2022d). Fourth, the effective connectivity with in particular the corresponding brain region contralaterally was high relative to other contralateral connectivities (Figs. S2 and S3), providing clear evidence that the effective connectivity algorithm could identify distant brain regions that could be expected to have high effective connectivity.

To test whether the vectors of effective connectivities of each of the 21 posterior parietal cortex regions with the 180 areas in the left hemisphere of the modified HCP atlas were significantly different, the interaction term was calculated for each pair of the 21 posterior parietal cortex effective connectivity vectors in separate 2-way ANOVAs (each 2×180) across the 171 participants, and Bonferroni correction for multiple comparisons was applied. The results were checked with the nonparametric Scheirer-Rey-Hare test (Scheirer et al. 1976; Sinha 2022).

Functional connectivity

For comparison with the effective connectivity, the functional connectivity was also measured at 7T with the identical set of participants, data, and filtering of 0.008–0.08 Hz. The functional connectivity was measured by the Pearson's correlation between the BOLD signal timeseries for each pair of brain regions, and is in fact the FC^{emp} referred to above. A threshold of 0.4 is used for the presentation of the findings in Fig. 5, for this sets the sparseness of what is shown to a level commensurate with the effective connectivity, to facilitate comparison between the functional and the effective connectivity. The functional connectivity can provide evidence that may relate to interactions between brain regions, while providing no evidence about causal direction-specific effects. A high functional connectivity may in this scenario thus reflect strong physiological interactions between areas, and provides a different type of evidence to effective connectivity. The effective connectivity is nonlinearly related to the functional connectivity, with

effective connectivities being identified (i.e. greater than zero) only for the links with relatively high functional connectivity.

Connections shown with diffusion tractography

Diffusion tractography can provide evidence about fiber pathways linking different brain regions with a method that is completely different to the ways in which effective and functional connectivity are measured, so is included here to provide complementary and supporting evidence to the effective connectivity. Diffusion tractography shows only direct connections, so comparison with effective connectivity can help to suggest which effective connectivities may be mediated directly or indirectly. Diffusion tractography does not provide evidence about the direction of connections. Diffusion tractography was performed on the same 171 HCP participants imaged at 7T with methods described in detail elsewhere (Huang et al. 2021). The major parameters were: 1.05 mm isotropic voxels; a 2 shell acquisition scheme with b-values = 1,000, 2,000 s/mm^2, repetition time/echo time = 7,000/71 ms, 65 unique diffusion gradient directions and 6 b0 images obtained for each phase encoding direction pair (AP and PA pairs). Preprocessing steps included distortion correction, eddy-current correction, motion correction, and gradient nonlinearity correction. In brief, whole brain tractography was reconstructed for each subject in native space. To improve the tractography termination accuracy in GM, MRtrix3's 5ttgen command was used to generate multitissue segment images (5tt) using T1 images, the segmented tissues were then co-registered with the b0 image in diffusion space. For multishell data, tissue response functions in GM, WM, and CSF were estimated by the MRtrix3' dwi2response function with the Dhollander algorithm (Dhollander et al. 2016). A Multi-Shell Multi-Tissue Constrained Spherical Deconvolution (MSMT-CSD) model with lmax = 8 and prior coregistered 5tt image was used on the preprocessed multishell DWI data to obtain the fiber orientation distribution (FOD) function (Smith 2002; Jeurissen et al. 2014). Based on the voxel-wise fiber orientation distribution, anatomically constrained tractography (ACT) using the probabilistic tracking algorithm: iFOD2 (2nd-order integration based on FOD) with dynamic seeding was applied to generate the initial tractogram (1 million streamlines with maximum tract length = 250 mm and minimal tract length = 5 mm). To quantify the number of streamlines connecting pairs of regions, the updated version of the spherical-deconvolution informed filtering of the tractograms (SIFT2) method was applied, which provides more biologically meaningful estimates of structural connection density (Smith et al. 2015).

The results for the tractography are shown in Fig. 6 as the number of streamlines between areas with a threshold applied of 10 to reduce the risk of occasional noise-related observations. The term "connections" is used when referring to what is shown with diffusion

Fig. 2. Effective connectivity *TO* the posterior parietal cortex (the rows) *FROM* 180 cortical areas (the columns) in the left hemisphere. The effective connectivity is read from column to row. Effective connectivities of 0 are shown as blank. All effective connectivity maps are scaled to show 0.15 as the maximum, as this is the highest effective connectivity found between this set of brain regions. The effective connectivity algorithm for the whole brain is set to have a maximum of 0.2, and this was for connectivity between V1 and contralateral V1. The effective connectivity for the first set of cortical regions is shown in the top panel; and for the second set of regions in the lower panel. Abbreviations: see Table S1. The four groups of posterior parietal cortex areas are separated by red lines. Group 1: the superior parietal cortex is above the top red line. Group 2: the intraparietal cortex is below the top red line. Group 3: the mainly somatosensory inferior parietal cortex regions is next. Group 4: the mainly visual inferior parietal cortex regions is below the lowest red line.

tractography, and connectivity when referring to effective or functional connectivity.

Results
Overview: effective connectivity, functional connectivity, and diffusion tractography

The effective connectivities *to* the posterior parietal cortex (PPC) from other cortical areas in the left hemisphere are shown in Fig. 2. The effective connectivities *from* the posterior parietal cortex to other cortical areas in the left hemisphere are shown in Fig. 3. The vectors of effective connectivities of each of the 21 parietal cortex regions with the 180 areas in the left hemisphere of the HCP-MMP1 atlas were all significantly different from each other. (Across the 171 participants the interaction term in separate 2-way ANOVAs for the comparisons between the effective connectivity of every pair of the 21 ROIs after Bonferroni correction for multiple comparisons were all $P < 10^{-90}$. The results were confirmed with the non-parametric Scheirer-Rey-Hare test (Scheirer et al. 1976; Sinha 2022)). The functional implications of the results described next are considered in the Discussion.

The 21 HCP-MMP cortical regions included as part of the posterior parietal cortex division considered here are grouped into 4 groups, based partly on the topology (with e.g. all area 7 regions together, then all intraparietal sulcus regions together); and also for especially

the inferior parietal regions guided by the Pearson's correlations between the effective connectivities of the 21 PPC regions from and to all 180 cortical areas in the left hemisphere, which are shown in Fig. S4, and by the corresponding correlations for the functional connectivities shown in Fig. S5. Fig. S4a shows the correlations between the rows shown in Fig. 2, and Fig. S4b shows the correlations between the columns shown in Fig. 3. These correlations are calculated using connectivity with areas outside the posterior parietal cortex.) The groups were as follows (see Table S1 for the list of brain regions, and Fig. 1 and Fig. S1 for their locations in the brain). Group 1, superior posterior parietal cortex: 7AL, 7 AM, 7PC, 7PL, 7Pm. Group 2, intraparietal sulcus cortex: AIP, LIPd. LIPv, MIP, VIP, IP0, IP1, and IP2. The inferior parietal PF and PG areas were divided just for ease of description into Group 3, PFcm, PFop, PFt, and PF (which include somatosensory system connectivity); with Group 4 consisting of PFm, PGi, PGs, and PGp (which include visual system connectivity) (Figs. S4 and S5). In the figures, these groups are separated by red lines. No analyses presented in the paper depend on this grouping.

To facilitate the description of the results, each of these groups is considered in turn, taking into account also the difference of the effective connectivities in the 2 directions for every link (Fig. 4), the functional connectivities (Fig. 5), and the diffusion tractography (Fig. 6). These groups are used to help present the findings, but different HCP-MMP regions within a group do not have identical
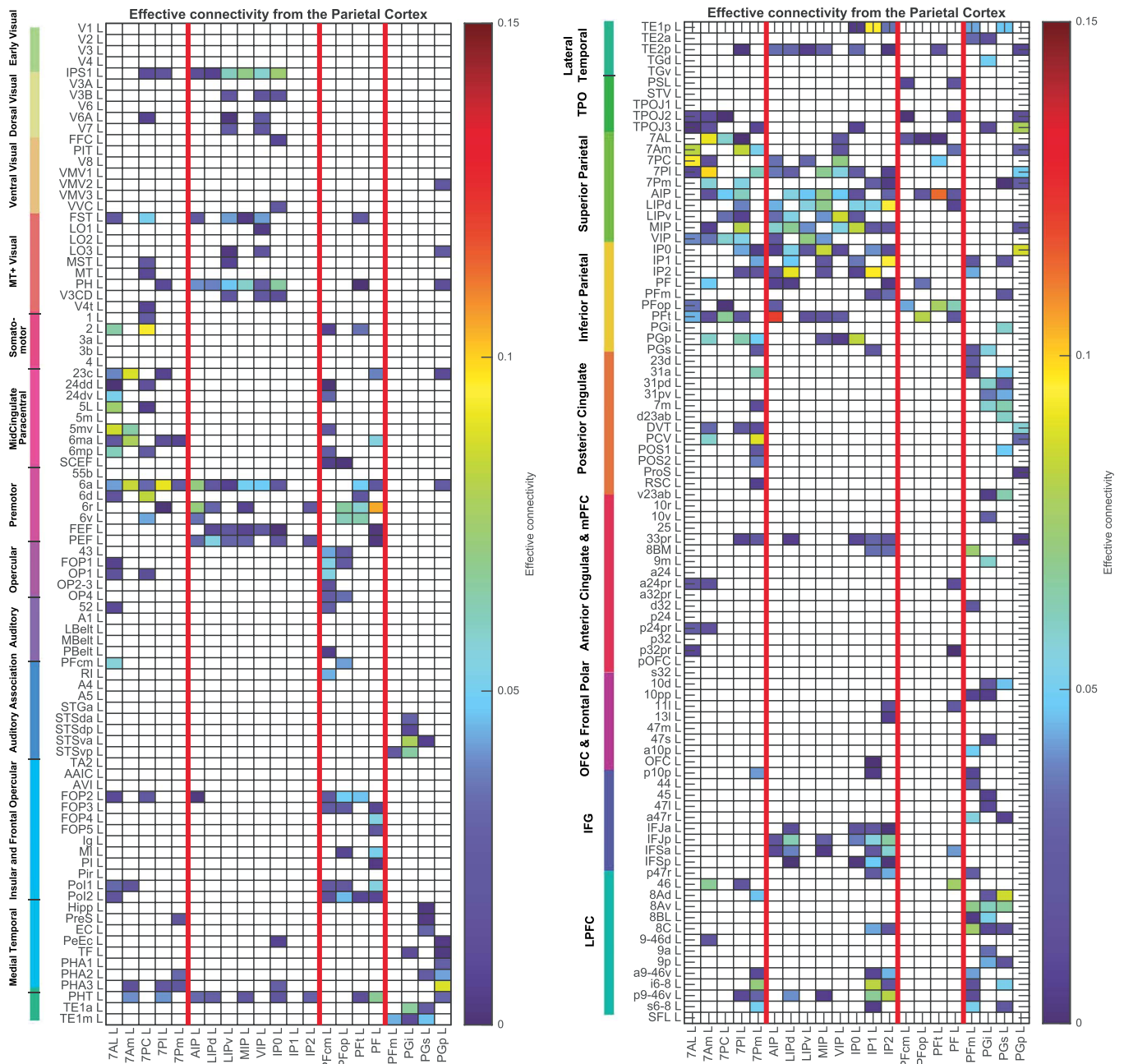
Fig. 3. Effective connectivity *FROM* the posterior parietal cortex *TO* 180 cortical areas in the left hemisphere. The effective connectivity is read from column to row. Effective connectivities of 0 are shown as blank. Abbreviations: see Table S1. The 4 groups of posterior parietal cortex areas are separated by red lines.

connectivity, and this shows part of the utility of the HCP-MMP atlas (Glasser, Coalson, et al. 2016a) and the approach taken here. The description starts with the left hemisphere, which is of especial interest as it is typically involved in language in humans, but there is a comparison with connectivity in the right hemisphere later.

Group 1, posterior superior parietal cortex, regions 7AL, 7Am, 7PC, 7PL, 7Pm, and relation to visuo-motor functions

As shown in Fig. 2, these regions have some inputs from early visual cortical areas including intraparietal sulcus area 1 (IPS1), V6A, and some MT+ complex regions,

FST, LO3, MST, MT, and V4t; major inputs from visual areas in the intraparietal sulcus including AIP, LIPd, LIPv, MIP, and VIP regions to especially 7PC and 7PL; somatosensory/motor connectivity (areas 1, 2, 5l, 5mv, 6ma, and 6mp); PHT (posterior inferior temporal cortex); some inputs from inferior parietal PF and PG; some inputs from the posterior cingulate cortex (including DVT, PCV, and RSC (Rolls, Wirth, et al. 2022)); from the supracallosal anterior cingulate cortex (p24pr, a24pr, 33pr), which is involved in aversive and somatosensory events (Rolls, Deco, et al. 2022c); and connectivity with the dorsolateral prefrontal cortex (including 46, i6–8, and 9–46d). In turn, there is effective connectivity
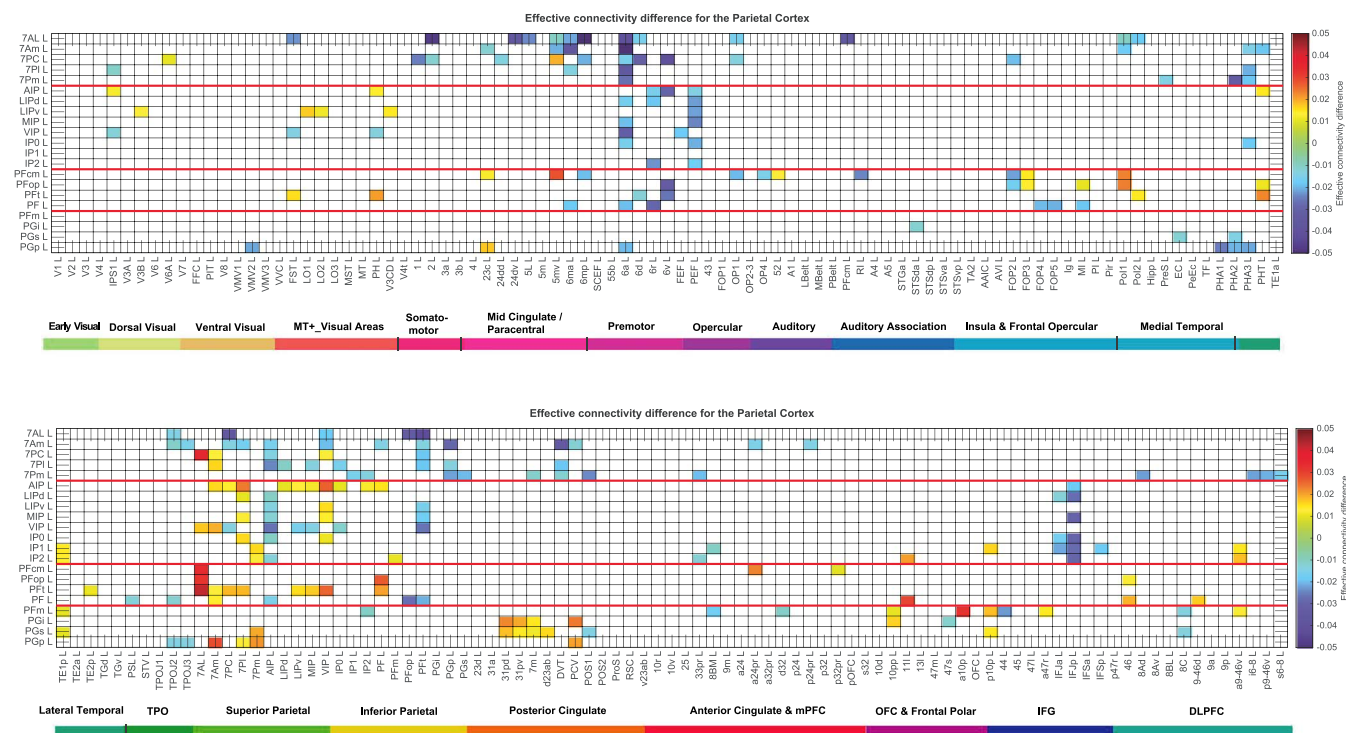
Fig. 4. Difference of the effective connectivity for the posterior parietal system with cortical areas. For a given link, if the effective connectivity difference is positive, the connectivity is stronger in the direction from column to row. For a given link, if the effective connectivity difference is negative, the connectivity is weaker in the direction from column to row. This is calculated from 171 participants in the HCP imaged at 7T. The threshold value for any effective connectivity difference to be shown is 0.01. The abbreviations for the brain regions are shown in Table S1, and the brain regions are shown in Fig. 1 and Fig. S1. The effective connectivity difference for the first set of cortical regions is shown in the top panel; and for the second set of regions in the lower panel.

from the posterior superior parietal cortex to many of these regions (Fig. 3), which in most cases is stronger from the posterior superior parietal cortex than to it (Fig. 3), apart from V6, VIP, and 5mv (Fig. 4). These area 7 regions also have effective connectivity directed to the hippocampal system, especially to the parahippocampal gyrus TH (PHA1–3) from the medial parietal areas 7Pm and 7Am (Figs. 3 and 4), to the temporo-parietal-occipital junction (TPOJ) regions, and to some inferior parietal cortex regions including PF and PGp.

The functional connectivity, which reflects correlations between brain regions and which may be less selective than effective connectivity which measures causal effects of one brain region on another, shows many similar connectivities, and emphases interactions with many early visual cortical areas and PHT and TE2p, with some auditory cortex regions such as PBelt and A4, and the hippocampal system including the presubiculum and parahippocampal TH regions PHA1–3 (Fig. 5).

The diffusion tractography (Fig. 6) is again largely consistent with the effective connectivity, though provides more indication of connections with early visual cortical areas, with auditory cortex, with the hippocampus and presubiculum, with TE1p, and with the posterior cingulate and related cortex especially the antero-dorsal regions, which include RSC, 31a, PCV, POS2, and POS1 involved in visuo-spatial functions (Rolls, Wirth, et al. 2022).

In terms of possible differences between the area 7 regions, the medial 7Pm region had less effective connectivity with somatosensory/premotor areas, and more with the posterior cingulate cortex especially PCV, POS2, and the retrosplenial cortex (RSC), which are in the antero-dorsal complex regions especially implicated in visuo-spatial functions (Rolls, Wirth, et al. 2022). This may be an interesting and telling difference in the connectivity of lateral vs medial posterior parietal area 7 regions, with the lateral areas more involved in somatomotor functions, and the medial area 7 regions more involved in visuo-spatial functions, which would be in line with minimizing connection length as a principle that influences the topology of the cerebral cortex (Rolls 2016).

Group 2, intraparietal posterior parietal cortex, regions AIP, LIPd, LIPv, MIP, VIP, IP0, IP1, and IP2

As shown in Fig. 2, these regions have strong effective connectivity from early visual cortical areas including dorsal visual intraparietal sulcus area 1 (IPS1), V3B, V6A, and V7; ventral visual FFC, and posterior inferotemporal PIT and PHT; from several MT+ complex visual regions including FST, LO1, LO3, PH, and V3CD; from premotor especially 6a, 6r and the premotor eye field PEF; strongly from visual anterior inferotemporal TE1p and TE2p; from area 7 regions; from inferior parietal regions including PGp; from the orbitofrontal cortex (medial regions, 11 and
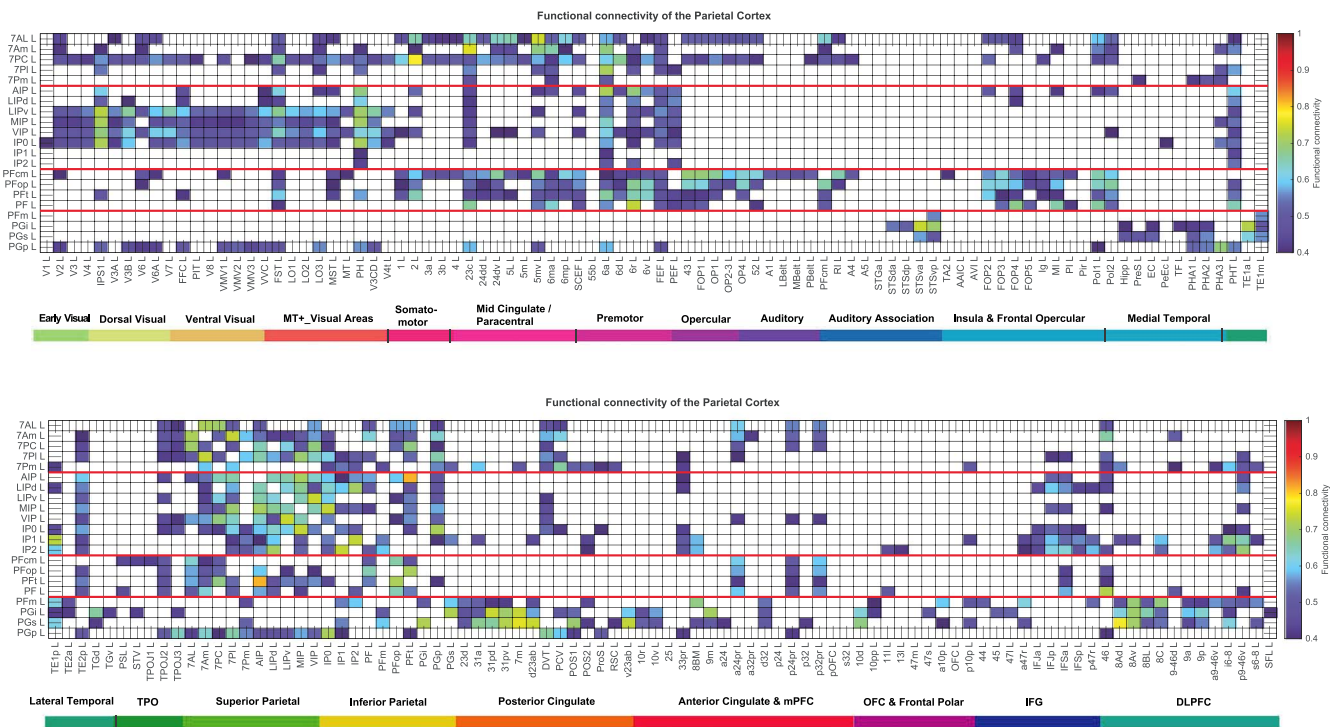
Fig. 5. Functional connectivity between the posterior parietal cortex and 180 cortical areas in the left hemisphere. Functional connectivities less than 0.4 are shown as blank. The upper Fig. shows the functional connectivity of the 21 parietal regions with the first half of the cortical areas; the lower Fig. shows the functional connectivity with the second half of the cortical areas. Abbreviations: see Table S1. The 4 groups of posterior parietal cortex areas are separated by red lines.

OFC); frontal pole p10p; from the inferior frontal gyrus; and extensively with the dorsolateral prefrontal cortex, especially 8C, a9–46v, i6–8, and p9–46v. Many of these connectivities are reciprocated (Fig. 3), but the effective connectivities are stronger to the intraparietal areas from early visual cortical areas, TE1p (to IP1 and IP2), area 7 regions, and the medial orbitofrontal cortex (Fig. 4), indicating that these are mainly input areas to the intraparietal regions. Conversely, the effective connectivities are stronger from the intraparietal areas to premotor areas (6a, 6r, and PEF); and to the inferior frontal gyrus regions (IFJ); and to the parahippocampal gyrus PHA (Figs. 3 and 4), providing evidence that these are output pathways from the intraparietal cortex.

The functional connectivity is consistent (Fig. 5), but indicates more interactions with early visual cortical areas including the ventromedial visual areas (VMV) implicated in scene perception (Sulpizio et al. 2020); with somatosensory/premotor cortical regions; with the hippocampal system; with TE1p and TE2p; with posterior cingulate/early visual DVT; and with supracallosal anterior cingulate 33pr and p24pr (Rolls, Deco, et al. 2022c).

The diffusion tractography (Fig. 6) is also consistent, and emphasizes connections with somatosensory/premotor cortical regions; shows some connections with auditory cortex; and with the posterior cingulate cortex especially the dorsal transitional visual area DVT implicated in scene perception (Sulpizio et al. 2020; Rolls, Wirth, et al. 2022).

Group 3, inferior parietal cortex, regions PFcm, PFop, PFt, and PF (connectivity with the somatosensory system)

Topologically (Caspers et al. 2008; Caspers and Zilles 2018), PG areas are posteriorly in the posterior parietal cortex, and the PF areas are more anterior (Fig. 7). In terms of alternative terminology in common use for the inferior parietal cortex, the angular gyrus BA 39 is posterior and may include HCP-MMP1 regions IP1, IP0, PGi, PGs, and PFm, and is implicated in memory and semantic processing, with damage on the left related to dyslexia and agraphia and on the right to body image (Davis et al. 2018). The supramarginal gyrus BA40 is mainly represented in the HCP-MMP1 by PF, PFt, and the PeriSylvian language area PSL and is related on the left to phonology and is part of the mirror neuron system (Caspers et al. 2008). The HCP-MMP1, based as it is on cortical thickness and myelination, functional connectivity, and task-related activations (Glasser, Coalson, et al. 2016a), thus provides a more detailed parcellation than BA 40 the supramarginal gyrus and BA 39 the angular gyrus.

PFcm

PFcm is close to opercular areas OP1–4, which are regions activated by vestibular stimulation, as is PFcm (Huber et al. 2022). As shown in Figs. 1–4 and Table S2, PFcm has effective connectivity with OP1–4, and with somatosensory cortical areas (5L, 5mv) and the somatosensory insula and frontal opercular areas
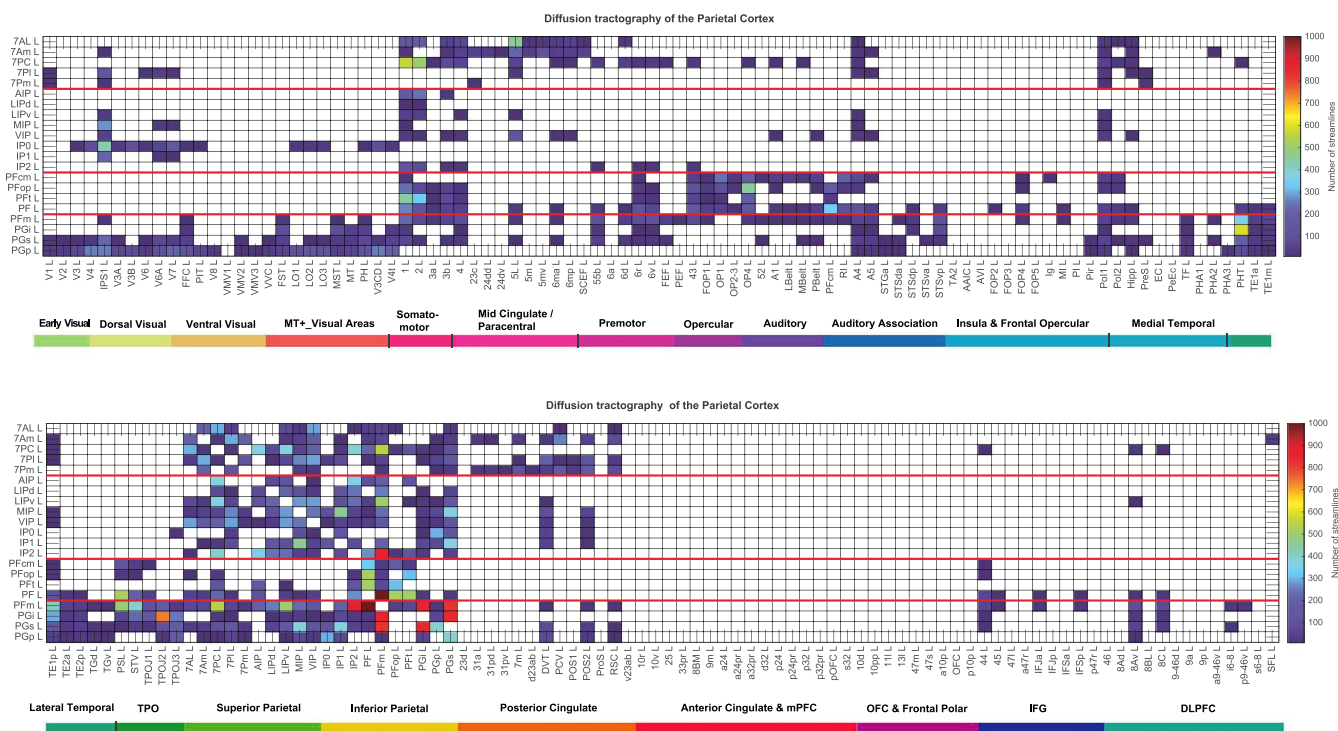
Fig. 6. Connections between the posterior parietal cortex and 180 cortical areas in the left hemisphere as shown by diffusion tractography using the same layout as in Figs. 2, 4 and 5. The number of streamlines shown was thresholded at 10 and values less than this are shown as blank. Abbreviations: see Table S1. The 4 groups of posterior parietal cortex areas are separated by red lines.

(FOP), from 7AL, with PFop, with the mid-cingulate cortex, and from the supracallosal (supracallosal, somatosensory/punishment-related (Rolls, Deco, et al. 2022c)) anterior cingulate (regions a24pr, p24pr, p32pr) cortex. The connectivity involving OP1–4, via PFcm, may provide for self-motion signals of vestibular origin to influence parietal processing in areas such as 7AL and PFop. It also has effective connectivity with TPOJ2 and with the PeriSylvian Language area (PSL), and with premotor cortical areas including the midcingulate cortex. As shown in Fig. 4, it tends to receive from somatosensory areas, and has connectivity to premotor 6mp. The functional connectivity provides in addition some evidence for interactions with some early visual cortical areas (Fig. 5), and the tractography provides in addition some evidence for connections with auditory areas.

PFop and PFt

These are also anterior parts of the inferior parietal cortex, adjoin somatosensory cortex (area 2 etc.), and have primarily somatosensory connectivity (Figs. 1–4 and Table S2). The somatosensory areas from which they receive effective connectivity include 2, frontal opercular FOP1–4, and insular cortex including the posterior insular cortex PoI1–2; and they have effective connectivity directed to premotor cortical areas (6d, 6v and mid-cingulate cortex) (Fig. 4). They also receive effective connectivity from the supracallosal anterior cingulate cortex (which responds to aversive stimuli including pain and which also projects to the midcingulate cortex (Rolls,

Deco, et al. 2022c)); and some input from posterior inferior temporal cortex PHT and also TE2p.

PFt (which is more dorsal) also receives effective connectivity from superior parietal (7Al, 7Am, 7PC and 7PL) and intraparietal (AIP, LIPv, MIP and VIP) regions, and so is implicated in visuo-motor as well as somatosensory functions. These regions have little effective connectivity with the orbitofrontal and dorsolateral prefrontal cortex. The functional connectivity (Fig. 5) is generally consistent though provides more indication of some interaction with early visual cortical areas; and the diffusion tractography (Fig. 6) is quite consistent with the effective connectivity.

PF

Region PF is relatively far anterior in the inferior parietal cortex, and relatively close to somatosensory areas and to the superior parietal cortex (Figs. 1 and 7a), and consistent with this and the principle of minimization of connection length (Rolls 2016), it has effective connectivity with somatosensory areas (e.g. FOP5, insula), premotor areas (e.g. 6ma and the mid-cingulate cortex), and visuo-motor areas in the intraparietal sulcus (e.g. AIP, LIPd) and in area 7 (7Am). However, it also has effective connectivity with the posterior inferior temporal visual cortex (PHT), with reward-related medial orbitofrontal cortex area 11l, and punishment-related supracallosal anterior cingulate cortex a24pr; with language-related areas (the PeriSylvian language (PSL) area and region 44 of Broca's area); and (also unlike PFop and PFt) with the dorsolateral prefrontal cortex (Figs. 2–4 and

Table S2). In terms of directionality (Fig. 4), the direction is towards PF from somatosensory area 5, from 7Am, and from the medial orbitofrontal cortex; and away from PF towards premotor 6a and 6r. The functional connectivity (Fig. 5) is consistent and shows a few more interactions including with region 44 of Broca's area; and the diffusion tractography (Fig. 6) reveals also some connections with somatosensory regions 1, 2, 3a and 3b, and the inferior temporal visual cortex. The implication is that PF combines information from the somatosensory system with inputs from visual and visuo-motor regions to form multimodal representations of shapes of felt objects and of the body, and sends outputs not only to premotor areas; but also very interestingly to a language-related area (PSL), with the diffusion tractography showing connections with Broca's area 44 and 45 (Fig. 6). The diffusion tractography also provides an indication of some connections with auditory cortex areas and with STS visual–auditory cortex.

Group 4, inferior parietal cortex, regions PFm, PGi, PGs, and PGp

These are the more posterior regions in the inferior parietal cortex (Fig. 1).

PFm

PFm is posterior to PF (Fig. 1), and in contrast is not a mainly somatosensory-influenced area with premotor output. Instead it has effective connectivity with high-order object-related areas (visual inferior temporal TE1m, TE1p, TE2a; auditory–visual superior temporal sulcus [STS]), receives from the frontal pole (a10p, p10p, 10pp) (implicated in planning and sequencing); receives from the reward-related medial orbitofrontal cortex (OFC) and the punishment/non-reward related lateral orbitofrontal cortex (a47r and p47r); and has effective connectivity with the reward-related pregenual anterior cingulate cortex (d32) (Figs. 2–4, Table S1). It also has effective connectivity with visuo-motor parietal areas including IP1 and IP2, and with PGs and the visuo-spatial part of the posterior cingulate cortex (23d, 31a (Rolls, Wirth, et al. 2022)). It also has extensive connectivity with the dorsolateral prefrontal cortex; and has connectivity with region 44 of Broca's area.

PGi

PGi is the most anterior/inferior PG region (Figs. 1 and 7b). It has effective connectivity with "what" (not visuo-spatial) systems including the inferior temporal visual cortex (TE1a, TE1m, TE2a) where objects are represented; with auditory–visual association cortex (STSva, STSvp, STSda, STSdp); with the temporo-parieto-occipital junction areas (TPOJ1–3) (which are activated during theory of mind processing (Buckner and DiNicola 2019; DiNicola et al. 2020)); with temporal pole TGd and TGv that are involved in semantic representations (Bonner and Price 2013); with PGs; with the frontal pole (10d, 10pp, a10p); with parahippocampal TF that is linked with ventral
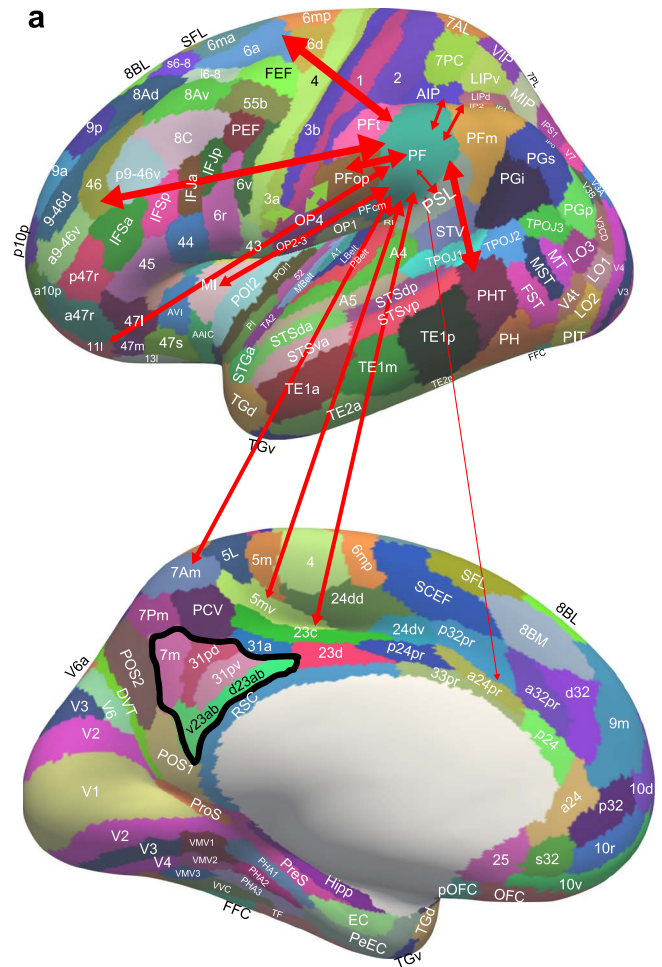
Fig. 7a. Effective connectivity of region PF. The widths of the red lines and the size of the arrowheads indicate the magnitude and direction of the effective connectivity with PF, which are shown in Table S2. The black outline encloses the postero-ventral memory-related regions of the posterior cingulate cortex. PF receives somatosensory inputs from many cortical regions including PFop which in turn receives from somatosensory 5 and fronto-opercular regions such as OP4 which in turn receive from somatosensory cortex such as 3a. (The green arrows help to illustrate the somatosensory hierarchy from for example 3a etc via OP4 to PFop to PF.) PF also receives some visual inputs from AIP, LIPd, IP2 and 7Pm. PF has outputs to premotor cortical areas (6) including the mid-cingulate cortex.

stream visual areas (Rolls, Deco, et al. 2022d); with the reward-related pregenual anterior cingulate cortex and with the nonreward-related lateral orbitofrontal cortex 47s; and with the postero-ventral part of the posterior cingulate cortex (31pd, 31pv, 7m, d23ab, v23ab), which is implicated in episodic memory (Rolls, Wirth, et al. 2022); and with the dorsolateral prefrontal cortex (Figs. 2–7b and Table S1). This connectivity implicates PGi in representations of objects and people relating to ventral stream temporal lobe visual and auditory processing, and linking them into memory systems via the posterior cingulate cortex. Consistent with this, the functional connectivity reveals some interactions with the hippocampal system (hippocampus, entorhinal cortex, parahippocampal TF and TH (PHA1–3) (Fig. 5). The tractography provides some evidence for connections with the PSL areas, and with Broca's area region 44 (Fig. 6).

Fig. 7b. Effective connectivity of region PGi. The widths of the lines and the size of the arrowheads indicate the magnitude and direction of the effective connectivity, which are shown in Table S2. 7Pm and IP1 connect to PGs which in turn connects to PGi, providing a route for PGi to receive visual motion information, and to connect that to areas such as STSda, STSva, STSdp and STSvp. The black outline encloses the postero-ventral memory-related regions of the posterior cingulate cortex, which connect to the hippocampal system (Rolls et al. 2022e).

Fig. 7c. Effective connectivity of region PGp. The widths of the lines and the size of the arrowheads indicate the magnitude and direction of the effective connectivity, which are shown in Table S2. PGp has effective connectivity from area 7 and intraparietal regions, and has effective connectivity directed to parahippocampal TH (PHA1-3). It is proposed that this provides a route for visuo-spatial parietal cortex regions involved in spatial coordinate transforms to provide the hippocampal system with information useful in the idiothetic (self-motion) update of hippocampal spatial representations of allocentric space. Consistent with this, PGp also receives from visual scene-related areas DVT (part of the retrosplenial scene area (Sulpizio et al. 2020)) and ventromedial visual cortex (VMV2).

PGs

PGs is posterior to PGi (and therefore closer to visual cortical areas), and is superior to PGp (Fig. 1). In contrast to PGi, PGs has connectivity with visuo-motor areas that are intraparietal (IP1) and in area 7 (e.g. 7Pm). It also has connectivity with object areas such as the visual inferior temporal cortex (TE1a, TE1m, TE1p) and with the Frontal pole (10d, a10p, p10p). It further has connectivity with the postero-ventral (memory-related) part of the posterior cingulate cortex, connectivity directed to the hippocampal memory system (hippocampus, entorhinal cortex, presubiculum, and parahippocampal PHA2) (Fig. 3), to PF and PGi, and with the dorsolateral prefrontal cortex (Figs. 2–6 and Table S1). The functional connectivity provides an indication in addition of some interactions with STS regions (Fig. 5), and the tractography is consistent with this and with some connections with TPOJ regions (Fig. 6).

PGp

PGp is a far posterior part of PG (Figs. 1, 7c and Fig. S1), and it has connectivity with some early visual cortical areas (e.g. VMV2 and LO3); and with intraparietal (e.g. MIP, VIP, IP0) and superior parietal 7 (e.g. 7Pm, 7PL, 7Pm) visuo-motor regions, both of which distinguish PGp from PGi and PGs and PFm. These connectivities contribute to the correlations shown in Figs. S4 and S5. However, PGp also has connectivity to parahippocampal TH areas PHA1–3 and with posterior cingulate DVT and ProS, all of which with VMV areas are implicated in visual scene processing (Sulpizio et al. 2020; Rolls, Wirth, et al. 2022; Rolls, Deco, et al. 2022d). PGp also has connectivity with TPOJ3 and TE2p, and has no connectivity with orbitofrontal cortex or prefrontal areas involved in short-term memory (Fig. 7c). The functional connectivity provides evidence for in addition interactions with early visual cortical

regions including other VMV regions, and with more intraparietal and area 7 regions (Fig. 5), and the diffusion tractography provides additional indications of this (Fig. 6). PGp may thus be involved in providing the hippocampal system with scene-related and visuo-motor including optic flow information, both of which may be useful for memory and navigation.

Effective connectivities of the posterior parietal cortex with contralateral cortical regions

The effective connectivities of the posterior parietal cortex from contralateral cortical areas are shown in Fig. S2, and to contralateral cortical areas in Fig. S3. The contralateral effective connectivities are in general weaker than those ipsilaterally. (The ratio across the matrices shown in Fig. 2 and Fig. S2 was that the contralateral effective connectivities were 62% of the ipsilateral effective connectivities.) Another feature of the effective connectivities is that they are strongest to the corresponding brain region contralaterally. (This is shown in the lower panel in Fig. S2 by the diagonal set of high effective connectivities from 7AL in the upper left to PFt, which reflect the effective connectivities to the corresponding contralateral region; and is also evident in Fig. S3.) This attests to the power of the effective connectivity algorithm, for it detects corresponding particular brain regions in the contralateral hemisphere. Also, this is an interesting principle of brain connectivity, which implies that the contralateral connectivities provide especially for comparison and support between regions performing similar processing in the other hemisphere, rather than providing for hierarchical computations between the two hemispheres.

Differences of effective connectivities of the right vs left hemisphere for the posterior parietal cortex

Most of the analysis presented so far have been for the left hemisphere, or of the left hemisphere with the right hemisphere. For completeness, the differences of effective connectivity for the Right *minus* the Left hemisphere for the parietal cortex regions are shown in Figs. S6 and S7. The differences between the hemispheres were overall small, but some differences are interesting to note. The general implication of what is shown in Figs. S6 and S7 is that the connectivities of many of these parietal regions are stronger in the right than the left hemisphere. This is consistent with the importance of the posterior parietal cortex in visuo-spatial and somatosensory processing, and in the role of the right hemisphere in spatial processing and probably in somatosensory and body image processing. Effective connectivities that are stronger in the left hemisphere include those of the posterior parietal cortex with the inferior temporal visual cortex (e.g. TE1p and TE2p) and with the hippocampal system.

Discussion

This is the first large-scale investigation across all 360 cortical regions in the HCP-MMP atlas of the effective connectivity of the posterior parietal cortex, with complementary evidence from functional connectivity and diffusion tractography analyses with the same 171 HCP participants. The same 7T data with identical preprocessing were used for the effective and functional connectivities. The focus of the discussion is on the implications for function of the connectivities of the different regions of the posterior parietal cortex described here. Some of the key findings are summarized in the "Conclusion and Overview" section at the end of the Discussion, and here the focus is on discussion of the implications of the findings for function.

Group 1, posterior superior parietal cortex, regions 7AL, 7Am, 7PC, 7PL, 7Pm: visuo-motor

The more posterior parts of this group (7PC, 7PL) receive inputs strongly from VIP, and from LIP and MIP (Fig. 2). Neurons in macaques in area VIP represent the direction and speed of visual motion (Colby et al. 1993), and may be useful in for example tracking moving visual stimuli, and encoding optic flow that can be useful in assessing self-motion and thereby in navigation. These neurons do not respond in relation to saccades. Neurons in macaques in LIP are active in visual, attentional, and saccadic processing (Gnadt and Andersen 1988; Colby et al. 1996; Munuera and Duhamel 2020). The ventral part of LIP (LIPv) has strong connections with two oculomotor centers, the frontal eye field and the deep layers of the superior colliculus, and may be especially involved in the generation of saccades (Chen, Li, et al. 2016b). The dorsal part (LIPd) may be more involved in visual processing, responding for example to visual targets for saccades (Chen, Li, et al. 2016b). Neurons in MIP (which may be the parietal reach region, PRR) are related to arm movement preparation and execution (Passarelli et al. 2021). They are implicated in the sensory-to-motor transformation required for reaching towards visually defined targets (Andersen 1995; Huang and Sereno 2018; Gamberini et al. 2020; Orban et al. 2021; Urgen and Orban 2021). 7PC and 7PL also have some inputs from early visual cortical areas including intraparietal sulcus area 1 (IPS1), V6A, MT, MST and LO3 and FST; somatosensory/premotor areas (regions 1, 2, 5, and 6); some inputs from inferior parietal PF and PG; some inputs from the posterior cingulate cortex (including DVT) (Rolls, Wirth, et al. 2022); from the supracallosal anterior cingulate cortex (p24pr), which is involved in aversive events (Grabenhorst and Rolls 2011; Rolls, Deco, et al. 2022c); and the dorsolateral prefrontal cortex (46 and 9–46d). Interestingly, there are also inputs from ventral visual stream regions including the posterior inferior temporal cortex PHT. Thus some information about the shape of objects reaches these regions, and that may be important for the control of grasping. In turn, there is effective connectivity from the posterior regions

of the superior parietal cortex to premotor cortical and somatosensory cortical areas (6, 5, see Fig. 3) and the midcingulate cortex, which in most cases is stronger from the posterior parietal cortex than to it (Fig. 4).

These area 7 regions therefore have connectivity that seems appropriate for making visually guided arm reach and grasp responses that are shaped properly because of shape inputs from the ventral visual system to seen objects. The more anterior parts of area 7 (7AL and 7Am) have more connectivity with somatosensory cortical areas (which are immediately anterior to them), and less with early visual cortical areas (Fig. 2), so may be involved more in proprioceptive and somatosensory integration than visuo-motor functions. 7Pm (which is medial) has connectivity with the nearby posterior cingulate regions DVT, POS1, and RSC, which are implicated in spatial including scene processing (Rolls, Wirth, et al. 2022). This may be an interesting and telling difference in the connectivity of lateral vs medial posterior parietal area 7 regions, with the lateral regions more involved in somatomotor functions, and the medial area 7 regions more involved in visuo-spatial functions, which would be in line with minimizing connection length as a principle that influences the topology of the cerebral cortex (Rolls 2016).

These area 7 regions also have effective connectivity directed to the hippocampal system, especially to parahippocampal gyrus TH (PHA2–3), and to the temporo-parietal-occipital junction area (TPOJ2–3) (Figs. 2–4).

The functional connectivity (Fig. 5) and diffusion tractography (Fig. 6) also provide evidence for some connectivity with auditory cortical areas, and this may be related to auditory cues being signals for orientation in space. They also provide further evidence for connectivity with the posterior cingulate cortex especially the antero-dorsal part involved in visuo-spatial functions (Rolls, Wirth, et al. 2022).

The area 7 parietal regions thus combine visuomotor with somatosensory functions, and the extensive research on these regions in macaques (Snyder et al. 1998; Gamberini et al. 2020; Orban et al. 2021; Passarelli et al. 2021) provides a guide to their functions in humans, including reaching for, grasping, and manipulating objects in space and tool use. These area 7 regions are also implicated in coordinate transforms from egocentric eye-based frames to allocentric world-based frames suitable for idiothetic update of hippocampal spatial representations (Andersen 1995; Snyder et al. 1998; Dean and Platt 2006; Vedder et al. 2017; Rolls 2020, 2021a). Consistent with this, vestibular as well as optic flow signals influence neurons in macaque 7a (Avila et al. 2019).

Group 2, intraparietal posterior parietal cortex, regions AIP, LIPd, LIPv, MIP, VIP, IP0, IP1, and IP2: visual motion

As noted above, neurons in macaques in area VIP represent the direction and speed of visual motion (Colby et al. 1993), and may be useful in for example tracking moving visual stimuli, and encoding optic flow which can be useful in assessing self-motion and thereby in navigation. These neurons do not respond in relation to saccades. Neurons in macaques in LIP are active in visual, attentional, and saccadic processing (Gnadt and Andersen 1988; Colby et al. 1996; Munuera and Duhamel 2020). The ventral part of LIP (LIPv) has strong connections with two oculomotor centers, the frontal eye field and the deep layers of the superior colliculus, and may be especially involved in the generation of saccades (Chen, Li, et al. 2016b). The dorsal part (LIPd) may be more involved in visual processing, responding for example to visual targets for saccades (Chen, Li, et al. 2016b). Neurons in macaque MIP (which may be the parietal reach region, PRR) are related to arm movement preparation and execution (Passarelli et al. 2021). They are implicated in the sensory-to-motor transformations required for reaching towards visually defined targets (Gamberini et al. 2020).

As shown in Fig. 2, these regions have strong effective connectivity from early visual cortical areas including from several MT+ complex visual regions in which neurons respond to global optic flow (Kolster et al. 2010; Galletti and Fattori 2018) (MST, FST, PH, and V3CD), intraparietal sulcus area 1 (IPS1), V3B, V6A (which is a visuo-motor region involved in grasping seen objects (Gamberini et al. 2020)), V7, and superior parietal area 7 regions involved in visuo-motor actions. These Group 2 intraparietal regions also receive in humans from ventral stream visual cortical areas including the fusiform face cortex (FFC), from inferior temporal cortex regions PIT, PHT, TE1p, and TE2p (Fig. 2). These ventral stream regions are likely to bring shape/visual form information (Rolls 2021b, 2021c; Rolls, Deco, et al. 2022a) to the intraparietal cortex regions important in shaping the hand to grasp and manipulate objects and tools. These Group 2 intraparietal regions also have connectivity with the inferior frontal gyrus and with the dorsolateral prefrontal cortex (especially 46, 8C, a9–46, i6–8, and p9–46v), which are likely to be important when there is a delay between the visual input and when the action can be performed (Funahashi et al. 1989). These connectivities are stronger to these prefrontal areas (Fig. 4), as is appropriate for the operation of short-term memory systems so that the memory does not dominate sensory inputs (Rolls 2016, 2021c). There is also connectivity directed towards the parahippocampal TH cortex (PHA3), which may be useful in providing information about visuo-motor actions to the hippocampal memory system (Rolls 2018; Rolls, Deco, et al. 2022d). There is also connectivity with the frontal pole p10p, which is likely to be important when sequencing and planning is involved in actions (Shallice and Burgess 1996; Gilbert and Burgess 2008; Shallice and Cipolotti 2018). The connectivity from the Group 2 intraparietal areas is strongly towards premotor cortical areas including especially 6a, and to the frontal eye field FEF and prefrontal eye field PEF (from especially AIP,

LIPd, LIPv, and VIP) (Fig. 4), which provides action-related outputs from these visuo-motor intraparietal regions. There is also connectivity especially for IP1 and IP2 from the orbitofrontal cortex (medial regions, 11l and OFC) which may provide reward feedback (Rolls 2019a, 2019c) of potential utility in learning whether actions made are correct, and with the frontal pole. There is also some connectivity with inferior parietal regions including PGp and PGs. Interestingly, this intraparietal part of the parietal cortex has relatively little effective connectivity with the posterior or anterior (or mid) cingulate cortex (Figs. 2–4), though in the right hemisphere IP1 has effective connectivity with 31a, d23ab, and POS2.

The functional connectivity is largely consistent (Fig. 5), but indicates more interactions with early visual cortical areas; with somatosensory/premotor areas; with the hippocampal system; with TE1p and TE2p, with posterior cingulate including DVT; and with supracallosal anterior cingulate 33pr and p24pr (Rolls, Deco, et al. 2022c). The diffusion tractography (Fig. 6) is also consistent, but suggests in addition connections with auditory cortex that may be useful in orienting gaze towards sounds.

The intraparietal cortical regions in humans thus are likely in terms of their connectivity (Figs. 2–6) to perform visuomotor functions (without somatosensory processing unlike area 7 regions), and the extensive research on these regions in macaques provides a guide to their functions in humans, including the control of eye movements to acquire and track visual stimuli given the outputs to the FEF and PEF. There are also outputs to regions 6a and 6r that might produce head and body movements to help stabilize images for the visual system. The output to the posterior inferior temporal visual cortex PHT is of interest, and might be involved in the stabilization of images for processing in later parts of the ventral visual system.

Group 3, inferior parietal cortex, regions PFcm, PFop, PFt, and PF: somatosensory/body processing supported by multimodal inputs

Topologically (Caspers et al. 2008; Caspers and Zilles 2018), PF areas are more anterior in the inferior parietal cortex, and the PG areas are more posterior (Fig. 7). In terms of alternative terminology in common use for the inferior parietal cortex, the supramarginal gyrus BA40 is mainly represented in the HCP-MMP1 (Glasser, Coalson, et al. 2016a) by PF, PFt, and the PSL area, and is related on the left to phonology, and is also part of the mirror neuron system which may be used to interpret the gestures and actions of other people (Caspers et al. 2008; Rizzolatti and Rozzi 2018). The angular gyrus BA 39 is posterior and may include HCP regions IP1, IP0, PGi, PGs, and PFm and is implicated in memory and semantic processing, with damage on the left related to dyslexia and agraphia and on the right to body image (Davis et al. 2018). The HCP-MMP1, based as it is on cortical thickness and myelination, functional connectivity, and task-related activations (Glasser, Coalson, et al. 2016a), thus provides a more

detailed parcellation than BA 40 the supramarginal gyrus and BA 39 the angular gyrus.

The PF areas (which are anterior in the inferior parietal cortex, and excluding PFm), as shown in Figs. 2 and 7a receive effective connectivity from somatosensory cortical areas (including 2, 5L, and 5mv), and have effective connectivities directed towards somatomotor premotor areas including 6ma, 6mp, 6a, 6d, 6r, and 6v and midcingulate premotor regions 23c, 24dd, and 24dv. The effective connectivities indicate that PF is at the top of a somatosensory hierarchy, with somatosensory inputs from especially PFop, frontal opercular 4 and 5, and the mid insula (Figs. 2 and 7a). PFop receives input from PFt and somatosensory Frontal Opercular FOP2–4, posterior Opercular OP4, 5 l and 5mv, and the insula (green in Fig. 7a). OP4 receive effective connectivity from somatosensory 1, 2, 3a, and 3b at the bottom of the somatosensory hierarchy (Fig. 7a). Thus part of the function of these PF areas may be related to somatosensory/body image and the sense of body ownership and of self that this bestows (Ronchi et al. 2018). The connectivity with the somatosensory insula and adjoining frontal operculum (FOP regions) (in which somatosensory responses are also found (Verhagen et al. 2004; Rolls et al. 2015)), further provides a foundation for understanding a function of the PF regions as involving body image, and indeed consistent with this, it has been argued that the insula is involved in the human awareness of feelings from the body (Craig 2011). Further than this, it has been shown that although somatosensory cortical areas 1–3 respond as much to the sight of touch as to the touch itself, the insula responds to the real touch only, and not to the sight of touch, which led to the proposal that the insula is involved in awareness that it is one's own body that is being touched, and not someone else's body (McCabe et al. 2008; Rolls 2010). This then fits with the concept that the PF PPC regions are involved in representing one's own body, and that anosognosia and other disorders of awareness of the body can be produced by PF damage in humans (Ronchi et al. 2018).

There is a clear transition of functionality from anterior to posterior within the PF regions. PFcm and PFop have mainly somatosensory inputs, and premotor outputs. PFcm has inputs from OP1–4, and is further implicated in responsiveness to vestibular inputs (Huber et al. 2022). Indeed, OP1–4 correspond approximately to the parieto-insular vestibular cortex (Grusser et al. 1990; Huber et al. 2022), and may make a contribution to heading direction useful for navigation (Chen, Gu, et al. 2016a). PFt (which is more dorsal, and closer to parietal visual areas) also receives effective connectivity from superior parietal (7Al, 7Am, 7PC, and 7PL) and intraparietal (AIP, LIPv, MIP, and VIP) regions, and so is implicated in visuomotor as well as somatosensory functions. Indeed, the combination of visual and somatosensory inputs is likely to be important for reaching with the correct shape of the hand to grasp an object, and when the object is felt that provides further information relevant to the action being performed. These regions (PFcm and PFop) also

receive inputs from the supracallosal anterior cingulate cortex, which is a region with somatosensory inputs that responds to many aversive stimuli (Grabenhorst and Rolls 2011; Rolls, Deco, et al. 2022c).

More posteriorly, and in a sense higher up the inferior parietal somatosensory hierarchy, PF (Fig. 7a) (which receives from PFop) also has somatosensory and premotor and visuo-spatial inputs relating to 7Am and intraparietal AIP, but adds to these, beyond what is found for earlier stages, strong effective connectivity from the posterior inferior temporal visual cortex (PHT, which is likely to introduce visual information about the shape of objects useful for performing actions on objects), from the reward-related medial orbitofrontal cortex 11l (which will provide reward-related information useful in building a semantic representation of felt objects and in influencing whether actions should be performed to obtain them), and, consistent with this concept, PF has effective connectivity directed towards language-related regions— the PeriSylvian language area (PSL), TPOJ2, STSvp (Rolls, Deco, et al. 2022b), and to prefrontal cortex areas involved in short-term memory related functions IFsa and 46 (Fig. 3). The diffusion tractography (Fig. 6) further emphasizes connections with language-related areas 44, 45, and PSL. PF also adds extensive connectivity to dorsolateral prefrontal areas 46, implicated in short-term memory (Goldman-Rakic 1996; Passingham 2021; Rolls 2021c), and appropriate for maintaining active during delays a memory of a tactile object.

PF may on this connectivity evidence (Fig. 7a) be the top of a somatosensory hierarchy that adds visual and reward inputs to form semantic representations of felt objects, which can then gain access to language systems, as well as having outputs to superior parietal and intraparietal areas involved in performing actions such as reach and grasping for felt or seen objects. PF may thus build a multimodal, semantic, representation of felt objects. The PSL region is very interesting, because it receives somatosensory inputs from PF, and has connections to STS semantic areas, so PSL may be a route for tactile inputs to become part of object representations (Rolls, Deco, et al. 2022b). All of the Group 3 somatosensory-related inferior parietal areas are conspicuous in not having effective connectivity with the posterior cingulate cortex and in having little connectivity with the hippocampal system.

Consistent with this connectivity, damage to the human inferior parietal cortex can result in tactile agnosia (also termed stereognosis), which is the inability to recognize objects through palpation in the absence of elementary sensory deficits (Klingner and Witte 2018). Recognition through the visual modality is preserved, and this aspect of semantics is suggested to rely on object/semantic representations in the temporal lobe (Rolls, Deco, et al. 2022b). The inferior parietal deficit can be interpreted as a failure of the associative-semantic system to match the tactile features identifying an object with its meaning (Berti and Neppi-Modona 2012; Berti et al. 2015).

The input to PF regions (mainly to PF) from anterior cingulate regions including a24pr, d32, p24pr; and orbitofrontal OFC, 11l (Fig. 2), which are involved in punishment and reward (Grabenhorst and Rolls 2011; Rolls 2019a, 2019b, 2019c; Rolls, Deco, et al. 2022c) deserves further consideration. It is found that the pleasantness and painfulness of touch is related to activations of the orbitofrontal cortex, whereas activations of somatosensory cortex are related to physical aspects of the stimuli such as their intensity (Rolls et al. 2003). Further evidence that the reward value of touch and related visual stimuli are not represented in parietal cortex is that "visual fixation neurons" (Mountcastle et al. 1975) do not reflect the reward value of visual stimuli measured by a devaluation experiment in which macaques were fed to satiety, and the neurons did not reverse the visual stimulus to which they responded when the reward value of the 2 stimuli was reversed in a visual discrimination task (Rolls et al. 1979). (This was tested following a visit to Vernon Mountcastle's lab in which he confirmed his view that reward value was represented by the parietal "command" neurons (Mountcastle et al. 1975).) Evidence that parietal neurons are related to decision-making (Platt and Glimcher 1999) does not contradict the hypothesis presented above, for the decision-making need not be about reward value but could be about the physical properties of the stimuli. Evidence about the fact that a stimulus is harmful could of course be useful in the parietal cortex to facilitate withdrawal, and about reward and punishment could be useful to provide evidence that an action has been successfully completed (or not), which could occur in the absence of a primary representation of the reward and painful affective value of touch, which appears to be in the human orbitofrontal and anterior cingulate cortex (Rolls et al. 2003; McCabe et al. 2008).

Group 4, inferior parietal cortex, regions PFm, PGi, PGs, and PGp: visual object and face motion analysis for social functions, theory of mind, memory, etc.

The PG areas, located posteriorly (Figs. 1 and 7b, c), and compared to PF areas, have more effective connectivity with visual cortical areas and have less connectivity than the Group 3 PF regions with somatosensory and premotor cortical areas. This fits with the location in the brain of the PG areas, and the importance of minimizing connection length in the brain, so that brain regions with many interconnections are found close together in the brain, where possible (Rolls 2016). However, the connectivity of PGi, PGs, PFm, and PGp are all quite different, suggesting different functions for each of these regions, so they are considered separately.

PGi

This most inferior part of the inferior parietal lobule is closest to ventral stream areas, and has connectivity with object/"what" brain regions including for vision the anterior inferior temporal TE1a, TE1m, TE1p, and TE2a; from all the STS auditory—visual association/semantic

areas; and from the anterior temporal lobe TG semantic areas (Bonner and Price 2013; Price et al. 2015) (Fig. 7b). It also has connectivity with the temporo-parieto-occipital junction region TPOJ3 implicated in semantic processing, theory of mind, and social behavior (Schurz et al. 2017; Buckner and DiNicola 2019; Quesque and Brass 2019; DiNicola et al. 2020). TPOJ regions and PGi are activated by faces (including face expression and other socially relevant visual representations (Patel et al. 2019)) vs other visual stimuli, as are the TE1a and STS regions that have effective connectivity with PGi (Yokoyama et al. 2021). It is important to recognize that regions in the STS include not only auditory responsiveness dorsally, but in much of the STS visual responsiveness, so STS regions should not be considered as only "auditory association cortex." Indeed, it was discovered that single neurons in the macaque STS respond to face expression and also to face and head movement to encode the social relevance of stimuli (Hasselmo, Rolls, and Baylis 1989a; Hasselmo, Rolls, Baylis, and Nalwa 1989b). For example, a neuron might respond to closing of the eyes, or to turning of the head away from facing the viewer, both of which break social contact (Hasselmo, Rolls, and Baylis 1989a; Hasselmo, Rolls, Baylis, and Nalwa 1989b). Some neurons respond to the direction of gaze (Perrett et al. 1987). It was assumed that some of the movement-related information required to account for the neuronal responses in the cortex in the STS came from the dorsal visual stream and could be combined in the STS with ventral stream information about the identity of the faces. It was found that many of the neurons in the STS respond only or much better to moving faces or objects (Hasselmo, Rolls, and Baylis 1989a), whereas in the anterior inferior temporal cortex neurons were discovered that responded well to static visual stimuli, and were tuned for face identity (Perrett et al. 1982; Rolls 1984; Hasselmo, Rolls, and Baylis 1989a; Rolls, Treves, and Tovee 1997b; Rolls, Treves, Tovee, and Panzeri 1997c; Rolls 2000; Rolls and Treves 2011). It is now proposed that PGi, with its inputs from PGs that has connectivity with superior parietal and intraparietal regions that encode visual motion, is part of this processing stream for socially relevant face-related information. Consistent with this, the effective connectivity is strong from PGi to STS regions, though there is some effective connectivity also from PGs and PFm to STS regions (Figs. 2–4 and 7b). In humans, representations of this type could provide part of the basis for the development of systems to interpret the social and emotional significance of such stimuli, including theory of mind. Consistent with this, PGi and PGs receive inputs from PCV (the precuneus visual area) and 7m that are regions of medial parietal cortex related to the precuneus (Rolls, Wirth, et al. 2022), which is implicated in visual and self-referential processing (Cavanna and Trimble 2006; Freton et al. 2014). Connectivity with the pregenual reward-related anterior cingulate cortex introduces reward value into this region, potentially useful in forming semantic

including social representations of objects and faces. Very interestingly, there is also connectivity with the postero-ventral parts of the posterior cingulate cortex (31pd, 31pv, 7m, d23ab, v23ab) that are implicated in episodic memory (Rolls, Wirth, et al. 2022), and with the hippocampal system (parahippocampal TF) and is thus likely to be involved in the memory-related functions of the inferior parietal cortex (Davis et al. 2018). Consistent with this, the functional connectivity reveals some interactions with the hippocampal system (hippocampus, entorhinal cortex, parahippocampal TF and TH (PHA1–3)) (Fig. 5). The tractography provides some evidence for connections with the PSL areas, and with Broca's area region 44 (Fig. 6). PGi also has very extensive connectivity with dorsolateral prefrontal cortex regions (8BL, 8Ad, 8Av, 9a, 9b, s6–8) implicated in short-term memory (Fig. 7b).

PGs

PGs is posterior to PGi (and therefore closer to visual cortical areas), and is superior to PGp (Fig. 1 and Fig. S7b). In contrast to PGi, PGs has connectivity with visuo-motor areas that are intraparietal (IP1) and in area 7 (e.g. 7Pm), but it does also (as PGi) have connectivity with object areas such as the visual inferior temporal cortex (TE1a, TE1m, TE1p) (Figs. 2–4). PGs also has connectivity with the Frontal pole (10d, p10p), regions implicated in planning and sequencing (Shallice and Burgess 1996; Gilbert and Burgess 2008; Shallice and Cipolotti 2018) and prospective as well as retrospective memory especially about the self (Underwood et al. 2015). It also has connectivity with the postero-ventral (7m, 31pd, 31pv, d23ab, d23ab) part of the posterior cingulate cortex, which has effective connectivity to the hippocampal episodic memory system (Rolls, Wirth, et al. 2022), and connectivity directly to the hippocampal memory system (hippocampus, entorhinal cortex, presubiculum, and parahippocampal PHA2) (Fig. 3), to PF and PGi, and with the dorsolateral prefrontal cortex (Figs. 2–6 and Table S1). The functional connectivity provides an indication in addition of some interactions with STS regions (Fig. 5), and the tractography is consistent with this and with some connections with TPOJ regions (Fig. 6). The effective connectivity from PGs to PGi (Fig. 3) may provide PGi with visual motion information, where it can be combined with object and face information. PGi in turn has connectivity to STS regions (Figs. 3 and 7b), and may provide a route for dorsal visual stream information to reach the STS areas where neurons often respond primarily to moving faces, heads, or objects (Hasselmo, Rolls, and Baylis 1989a; Hasselmo, Rolls, Baylis, and Nalwa 1989b). Consistent with this, PGi does have strong effective connectivity (e.g. 0.078) to STSda, STSdp, STSva, and STSvp.

PFm

PFm is not a somatosensory area (unlike other PF areas). PFm receives from high order visual (TE1m, TE1p, TE2a) and visual/auditory (STSvp) areas that represent objects

and faces and (for the STS) their motion and expression (Hasselmo, Rolls, and Baylis 1989a). It has some intraparietal visuo-motor inputs (IP1 and IP2), and has connectivity with the visuo-motor (dorsal/anterior) parts of the posterior cingulate cortex (23d, 31a) and not the memory related parts; it also receives from the frontal pole (a10p, p10p, and 10pp); and it has effective connectivity with the reward related regions (orbitofrontal cortex OFC and pregenual anterior cingulate d32) and punishment-related orbitofrontal cortex a47r (Grabenhorst and Rolls 2011; Rolls, Deco, et al. 2022c). PFm thus appears to be a part of the parietal cortex that communicates with the visuo-spatial part of the posterior cingulate cortex (Rolls, Wirth, et al. 2022), and could thereby reach the hippocampus for visuo-spatial functions. In particular, the retrosplenial complex in the posterior cingulate cortex visuo-spatial part is especially important with respect to the location of landmarks (Persichetti and Dilks 2019); and posterior cingulate area 31 is implicated by neuroimaging in representing heading direction (Baumann and Mattingley 2021). A small region in the parieto-occipital sulcus (POS) that has been considered in connection with the posterior cingulate cortex (Rolls, Wirth, et al. 2022) has also been described as in the medial parietal cortex directly anterior to the visually scene-selective medial place area (Silson et al. 2016), and has strong functional connectivity with anterior portions of the scene-selective parahippocampal place area (Epstein 2008) (aPPA), located in the medial temporal cortex. This connectivity-defined region overlaps with regions of the medial parietal cortex engaged during memory recall, and there may be distinct regions for people and places (Silson et al. 2019). PFm has extensive connectivity with the dorsolateral and infer-olateral prefrontal cortex regions (Figs. 2 and 5), and is likely to be involved in short-term memory, which plays a key role in top-down attention by providing the continuing top-down bias for biased competition in the cortical regions linked to these prefrontal cortical areas enabling attentional interactions between the spatial and object streams (Deco and Rolls 2005a; Deco and Rolls 2005b; Rolls 2016, 2021c). PFm thus appears to combine visual motion with temporal lobe object/face information, and has connectivity with posterior cingulate areas involved in scene (/place) processing. It also has connectivity with language-related areas (Broca's area 44).

PGp

PGp is a far posterior part of PG (Figs. 1, 7c and Fig. S1), and it has effective connectivity with some early visual cortical areas related to scene processing (e.g. VMV2 and LO3) (Kamps et al. 2016; Sulpizio et al. 2020; Rolls, Deco, et al. 2022d); and with intraparietal (e.g. MIP, VIP, IP0) and superior parietal 7 (e.g. 7Pm, 7PL) visuo-motor regions, both of which distinguish PGp from PGi and PGs and PFm (Fig. 7c). These effective connectivities contribute to the correlations shown in Figs. S4 and S5. However, PGp also has connectivity to parahippocampal TH areas PHA1–3 and with posterior cingulate DVT and ProS, all of which

with VMV areas are implicated in visual scene processing (Sulpizio et al. 2020; Rolls, Wirth, et al. 2022; Rolls, Deco, et al. 2022d). Functional connectivity between PGp in the human angular gyrus and the parahippocampal scene area, hippocampus, and retrosplenial complex (Boccia et al. 2017) is consistent with and supports what is described here and elsewhere (Rolls, Wirth, et al. 2022). PGp also has connectivity with TPOJ3 and TE2p, and has no connectivity with the orbitofrontal cortex, or with prefrontal areas involved in short-term memory. The functional connectivity provides evidence for, in addition, interactions with early visual cortical regions including other VMV regions, and with more intraparietal and area 7 regions (Fig. 5), and the diffusion tractography provides additional indications of this (Fig. 6). The connectivity of PGp, because it has connectivities with scene and ego-motion regions, and with the parahippocampal cortex in which spatial view cells are found (Rolls, Robertson, and Georges-François 1997a; Robertson et al. 1998; Rolls et al. 1998; Georges-François et al. 1999; Wirth et al. 2017; Rolls and Wirth 2018; Tsitsiklis et al. 2020), implicates PGp in navigation (Rolls 2020, 2021a). PGp may be involved together with its connected intraparietal regions in the coordinate transforms necessary to map from retinal inputs to scenes which require representations of these types (Rolls 2020, 2021a).

It is thus proposed that PGp provides a route for visuo-spatial parietal cortex regions involved in spatial coordinate transforms (Snyder et al. 1998; Rolls 2020) to provide the hippocampal system with information useful in the idiothetic (self-motion) update of hippocampal spatial view representations of allocentric space (Robertson et al. 1998; Wirth et al. 2017; Rolls and Wirth 2018; Rolls 2021a, 2022a, 2022b). Consistent with this, PGp also receives from visual scene-related areas (Sulpizio et al. 2020) DVT and ventromedial visual cortex (VMV2) (Fig. 7c).

Supporting evidence is that the caudal inferior parietal lobule (cIPL, which includes PGp) has functional connectivity with the anterior part of the parahippocampal place (or scene) area (Baldassano et al. 2016), and although not strongly responsive to standard scene localizers showing sequences of unfamiliar and unrelated scene images (Baldassano et al. 2016; Sulpizio et al. 2020), cIPL is activated by familiar places. For example, cIPL is involved in memory for visual scenes (Montaldi et al. 2006; Takashima et al. 2006; Elman et al. 2013; van Assche et al. 2016), object-place associations in a virtual reality environment (Burgess et al. 2001), and imagining past events or future events in familiar places (Hassabis et al. 2007; Szpunar et al. 2009).

Supporting evidence from macaque neuroanatomy

Although there are great developments of especially the human inferior parietal cortex, it is helpful to consider the evidence from macaque neuroanatomy and

connectivity (Cavada and Goldman-Rakic 1989a, 1989b; Neal et al. 1990; Morris et al. 1999; Margulies et al. 2009; Gamberini et al. 2020; Giarrocco and Averbeck 2021; Passarelli et al. 2021; Foster et al. 2021), which is consistent with the new findings in humans described here. For example, macaque VIP may have developed in humans into three subregions coding the head or self in the environment, visual heading direction, and the peripersonal environment around the head (Foster et al. 2022). In another example, superior parietal areas with visuo-motor functions connect with superior prefrontal cortex areas such as 8b, 9, and 46d and superior premotor areas such as F6 and F7, while inferior parietal areas such as PF with somatosensory functions connect with ventral premotor areas such as F4 and F5 (Giarrocco and Averbeck 2021). Macaque 7b, the anterior inferior part of the macaque parietal cortex including PF regions, has connections with somatosensory-related areas, including S1, S2, the vestibular cortex, area 5, and the insular cortex (Jones and Powell 1970; Cavada and Goldman-Rakic 1989b).

Area V6A in the macaque is a visual-somatosensory area that occupies the posterior part of the dorsal precuneate cortex (Gamberini et al. 2020; Gamberini et al. 2021). It represents the upper limbs and is involved in the control of goal-directed arm movements (Fattori et al. 2017). Macaque V6A hosts the so called "real-position cells," that is visual cells that encode spatial position in head-based (craniotopic) coordinates not in retinotopic coordinates (Galletti et al. 1993). Area V6A is strongly connected with prestriate visual areas, with superior parietal areas as shown here for humans, and with the premotor frontal cortex representing arm movement (Gamberini et al. 2021). Macaque V6A is divided into 2 subareas that together are involved in the visual and somatosensory aspects of "reach-to-grasp": V6Av that is more visual and V6Ad that is more somatosensory (Gamberini et al. 2018). The human homolog of V6Av has been identified in the posterior, dorsal-most part of precuneate cortex (Pitzalis et al. 2013; Pitzalis et al. 2015; Tosoni et al. 2015), in a territory probably included in the DVT region of the HCP-MMP1 atlas (Glasser, Coalson, et al. 2016a) and which (like macaque V6Av) is activated by optic flow (Pitzalis et al. 2013).

Another part of the macaque dorsal precuneate region includes the medial portion of area PEc (Gamberini et al. 2020). Area PEc is a visual-somatosensory area that represents both upper and lower limbs and is probably involved in locomotion and in the analysis of related optic flow (Raffi et al. 2011; Gamberini et al. 2020). Area PEc is strongly connected with part of posterior cingulate cortex 31, area 7m, and retrosplenial cortex (Bakola et al. 2010). Recently, the human homolog of PEc has been identified in the dorsal-most part of the precuneate cortex (Pitzalis et al. 2019; Di Marco et al. 2021; Maltempo et al. 2021), and may correspond to 7Am in the HCP-MMP1 atlas.

Relation of posterior parietal cortex regions to memory and navigation

Regions PGs and PGi have connectivity that links them to memory and they have strong connectivity with each other. PGs has effective connectivity directed primarily towards the hippocampal system, including the hippocampus, entorhinal cortex, parahippocampal cortex TH (PHA2), and the presubiculum, which is involved in episodic memory (Dere et al. 2008; Ekstrom and Ranganath 2018; Rolls 2018, 2021c, 2022b). Consistent with this memory-related function, PGs and PGi also have strong effective connectivity directed to the posterior, memory-related, parts of the posterior cingulate cortex (7m 31pv, 31pd, d23ab, and v23ab), which in turn have connectivity with the hippocampus and related regions such as the entorhinal cortex (Rolls, Wirth, et al. 2022)). PGs receives strong inputs from the frontal pole p10p implicated in planning and sequencing (Shallice and Burgess 1996; Gilbert and Burgess 2008; Shallice and Cipolotti 2018) and prospective as well as retrospective memory (Underwood et al. 2015); and has connectivity with 7Pm, intraparietal IP1 and temporo-parieto-occipital region TPOJ3 that may introduce visuo-spatial input. PGs may thus allow visuo-spatial input and planning/sequencing inputs to reach the hippocampal system to contribute to memory and navigation. PGs also receives input from inferior temporal visual TE areas, and is a brain region where visual motion signals may combine with object and face information.

PGi has somewhat different connectivity (Fig. 7b). Inputs to PGi come from auditory–visual association STS cortical areas, as well as from inferior temporal (TE1p, TE1m and TE2a) "what" systems; TPOJ1–3; from reward-related regions (vmPFC 10v and 10d, and pregenual anterior cingulate 9m and d32 (Rolls, Deco, et al. 2022c), and from PGs. It has effective connectivity to the posterior, memory related, parts of the posterior cingulate cortex (31pd 31pv 7m d23ab v23ab) through which it may influence the hippocampus (Rolls, Wirth, et al. 2022). PGi thus provides a parietal cortex route for object STS auditory/visual representations related to face expression etc., and reward-related inputs to reach the posterior part of the posterior cingulate cortex (Rolls, Wirth, et al. 2022), and thus the hippocampal memory system. Both PGi and PGs have extensive effective connectivity with the dorsolateral prefrontal cortex, which will enable contributions to short-term memory and top-down attention.

Region PGp (Fig. 7c) may relate to memory and navigation too, primarily via its effective connectivity directed to the parahippocampal TH cortex PHA1–3, which is involved in visual scene-based representations with the ventromedial VMV visual areas (Sulpizio et al. 2020). The inputs to PGp come from early ventral visual stream regions (e.g. VMV2) implicated in scene processing, and dorsal stream visual areas (MIP, VIP, IP0, 7Pm, 7PL, and 7Pm) implicated in self-motion processing,

and with them is likely to be involved in the visuomotor transforms from retinal to head-based to eventually world-based coordinate transforms that are important in idiothetic (self-motion) update of spatial representations (Andersen 1995; Snyder et al. 1998; Rolls 2020) that are important in memory and navigation when the view details are obscured (Rolls 2021a). Indeed, hippocampal and parahippocampal spatial view cells which are important in memory and navigation (Rolls and Wirth 2018; Rolls 2021a) may be updated idiothetically via these parietal brain regions PGp, 7, and the intraparietal visual cortical regions (Rolls 2020, 2022a, 2022b). These PG areas, and also PFm, may thus be involved in memory and navigation.

In more detail, it is proposed that the connectivity of the hippocampal system with the parietal cortex via PGp is involved in the idiothetic update of hippocampal spatial view cells (Robertson et al. 1998; Georges-François et al. 1999; Rolls and Wirth 2018; Rolls 2020, 2021a, 2022a). In contrast it is proposed that the inputs to the hippocampal system from the ventromedial visual areas VMV1–3 and parahippocampal gyrus where the parahippocampal scene (or place) area (Epstein and Kanwisher 1998; Epstein 2005; Epstein 2008; Epstein and Julian 2013; Kamps et al. 2016; Epstein and Baker 2019; Sulpizio et al. 2020; Natu et al. 2021) is located (Sulpizio et al. 2020) are part of the ventromedial visual stream (Rolls, Deco, et al. 2022a) that combines features to form scene representations implemented by spatial view cells in the parahippocampal gyrus and hippocampus (Stringer et al. 2005; Rolls et al. 2008; Rolls 2022a; Rolls, Deco, et al. 2022d). Thus, it is proposed that there are (at least) two "where" systems that relate to the hippocampal system, memory, and navigation. One "where" system involves the dorsal visual system to the parietal cortex and is used for idiothetic update of spatial view cells (Rolls, Deco, et al. 2022a). The other "where" system involves the ventromedial visual stream (Rolls, Deco, et al. 2022a) and is used for the combinations of visual features that when overlapping and locked together by associative learning to form a continuous attractor network can encode a visual scene (Stringer et al. 2005; Rolls et al. 2008) using spatial view cells in the parahippocampal scene (or place) area referred to above, which in turn connects to the hippocampus (Rolls, Deco, et al. 2022d).

An important type of neuron found in the primate hippocampus is whole body motion neurons, some of which respond to linear and others to rotational motion, and some of which respond to vestibular inputs, others to visual inputs for motion, and some to both (O'Mara et al. 1994). These neurons are probably involved in navigation especially when the view details are obscured, that is, idiothetic navigation (O'Mara et al. 1994; Rolls 2020, 2021a). (The rodent equivalent is probably "speed cells" (Kropff et al. 2015).) Macaque hippocampal whole body motion neurons may receive their vestibular inputs at least in part via the antero-dorsal part of the posterior cingulate cortex in that this region receives from PFm

which in turn may be influenced by PFcm and thus opercular areas OP1–4 which are part of the parieto-insular vestibular cortex PIVC, and in macaques there are neurons in a dorsal PCC region (and to a smaller extent in the retrosplenial cortex) that respond to vestibular inputs (Liu et al. 2021).

These inferior parietal visual areas, and especially PGi, also provide a route for visual motion information from the superior and intraparietal regions to be combined with object and face information to contribute to the responses of neurons in the STS to moving objects and faces. Consistent with this, it is suggested that PGs and PGi are involved in biological motion (Baker et al. 2018).

Relation of posterior parietal cortex regions to somatosensory including body image processing

PFop and PFt have similar connectivity, with strong effective connectivity from somatosensory region 2, the frontal opercular FOP1–4, and insular cortex including the posterior insular cortex PoI1–2; and they have effective connectivity directed to premotor cortical areas (6d, 6v, and mid-cingulate cortex) (Fig. 4). There is also some input from the supracallosal anterior cingulate cortex (which responds to aversive stimuli including pain and which also projects to the midcingulate cortex (Rolls, Deco, et al. 2022a)); and some input from posterior inferior temporal visual cortex PHT and also TE2p), from 7AL and from auditory PFcm. PFop is thus mainly somatosensory in terms of its connectivity, but PFt (which is more dorsal) also receives effective connectivity from superior parietal (7Al, 7Am, 7PC, and 7PL) and intraparietal (AIP, LIPv, MIP, and VIP) regions, and so is implicated in visuo-motor as well as somatosensory functions, and is therefore likely to be important in tool use (Baker et al. 2018).

PF (Fig. 7a) has effective connectivity with somatosensory areas (e.g. FOP5, insula), premotor areas (e.g. 6ma and the mid-cingulate cortex), and visuo-motor areas in the intraparietal sulcus (e.g. AIP, LIPd) and in area 7 (7Am). However, it also has effective connectivity with the posterior inferior temporal visual cortex (PHT), with reward-related medial orbitofrontal cortex area 11l, and punishment-related supracallosal anterior cingulate cortex a24pr; with language-related areas (the PSL area and region 44 of Broca's area; and (also unlike PFop and PFt) with the dorsolateral prefrontal cortex (Figs. 2–4 and Table S2). The implication is that PF combines information from the somatosensory system with inputs from visual and visuo-motor regions to form multimodal representations of shapes of felt objects, and sends outputs not only to premotor areas; but also very interestingly to a language-related area (PSL), with the diffusion tractography showing connections with Broca's area 44 and 45 (Fig. 6). The diffusion tractography also provides an indication of some connections with auditory cortex areas and with STS visual-auditory-semantic cortex. The connectivity of PF thus suits it for building multimodal representations *especially when the somatosensory system*

is involved, which could reach the semantic level in that there is connectivity with language areas (Rolls, Deco, et al. 2022b). Consistent with this, it is suggested that PF is involved in action observation and imitation, and tool use (Baker et al. 2018).

Relation of posterior parietal cortex to multimodal representations and language

The following concept is proposed based on the connectivity of the parietal regions including PGi and its topological position in the brain as shown in Fig. 7b. PGi is at the posterior end of a highly connected set of cortical areas extending from it towards the temporal lobe, including the TPOJ regions, the PeriSylvian language area (PSL), the ventral parts of STS regions with also links into visual object processing in inferior visual temporal TE regions, and reaching the temporal pole areas TGd and TGv. PGi is thus in a sense at one end of this great ventral processing system for what can be computed from visual object and auditory object representations, which can be combined in the STS regions for they receive from both visual TE and auditory regions in the superior temporal gyrus. In this system, multimodal representations can be built, that are likely to include all the visual and auditory properties of objects, and it is proposed that their visual motion information may be communicated to the STS regions in part from PGi (and to a smaller extent PFm and PGs, both of which connect with intraparietal regions and with STS regions). These properties might include the sight of a person, the sound of their voice, and also inputs from reward and punishment-representing systems in the orbitofrontal and anterior cingulate cortex. Thus this set of brain regions seems ideally suited with their connectivity to form what are described as semantic representations of objects, that is the properties of objects (Rolls, Deco, et al. 2022b). This could provide the basis for much social behavior, given the neuronal responses to face expression and face and head movement discovered in the macaque STS (Hasselmo, Rolls, and Baylis 1989a; Hasselmo, Rolls, Baylis, and Nalwa 1989b). The ventral stream areas described from TG to PGi, which include information about object and face motion can thus be seen as a system for building representations of objects etc. in the external world, based on visual and auditory inputs that are the key modalities in humans and other primates by which information from the world "out there" is received. This seems to be what the temporal lobes and the connected PG areas provide for. The PG contributions are important partly because the motion information is of the dynamic type that needs to be matched with the auditory information that has the same temporal time scale. For example, some of the neurons in the cortex in the STS that respond to face movements such as closing of the eyelids (Hasselmo, Rolls, and Baylis 1989a; Hasselmo, Rolls, Baylis, and Nalwa 1989b) are exquisitely tuned to for example the sight of mouth movements made while humans speak, and are ideal for association with the auditory inputs reaching

the same cortical STS regions to provide for cross-modal facilitation.

However, the connections of the PGi with the STS semantic regions are bidirectional. It is proposed that this provides a route for language-related semantic information from the cortex in the STS (Rolls, Deco, et al. 2022b) to gain access to visual parts of the parietal lobe, and then going posterior and superior to PGi and PGs to reach areas involved in the control of eye movements. This could provide a route important in reading, by providing for ongoing semantic decoding in the STS and TG to influence eye movements to the next part of a word, or the next words. This could relate to the dyslexia that can be produced by parietal lobe damage (Davis et al. 2018).

What seems to be missing so far in the PGi part of this system is information about the somatosensory properties of objects, and how the objects can be manipulated, perhaps as tools, under visual control. And of course any information from the somatosensory system is quite different in kind from most of what is represented in the temporal lobes, for the somatosensory system involves touch to the body or the position of the body, which is not a property that needs to be taken into account by the temporal lobe analysis of objects "out there" in the world. The solution proposed for the conundrum of whether PGi is a multimodal region appropriate for visual, auditory, and somatosensory convergence is that it is not the solution to the problem, for in terms of its connectivity described here PGi is primarily visual and auditory (Fig. 7b). However, the other "top" part of the inferior parietal cortex for somatosensory processing is PF (Fig. 7a), and this does not have major visual inputs. So where is all of the relevant information for multimodal visual, auditory, and somatosensory, and visuo-motor "action" information represented in the brain? Analysis of the effective connectivities measured as part of this research between the 360 cortical regions is that a key region for multimodal convergence is the set of TPOJ1–3 regions, which are highly connected with each other, and which between them have effective connectivities with all the major systems just described, including visual, auditory, STS, PF, and PGi. The implication is that in terms of connectivity the TPOJ and the nearby highly connected regions such as the PSL region and Superior Temporal Visual (STV) region are where semantic representations involving all of these properties are built in the brain (Rolls, Deco, et al. 2022b). There is an interesting contrast here with TG areas of the brain, which are likely to form multimodal "semantic" representations, but primarily based on visual and auditory properties of objects, which is primarily what are represented in the temporal lobes (Rolls 2021c; Rolls, Deco, et al. 2022b).

The proposal that the TPOJ and its nearby and highly connected PSL etc. regions are the key regions for semantic representations for all modalities is central to understanding language systems in the brain, for semantics is of course a key component of language, and the TPO regions have major effective connectivity

with language-related cortical areas including the PSL area, and Broca's area 44 and 45 (Rolls, Deco, et al. 2022b). How do these language areas relate to this computational system? It has been proposed that semantic representations in regions such as TPOJ and the PSL bias sequentially linked series of attractor networks in Broca's area and nearby inferior frontal gyrus regions to transform semantic representations into speech production (Rolls and Deco 2015). The model of how this might be done utilizes serially coupled attractor networks each biased by the semantics to produce the sequence that is grammatical in a learned language (Rolls and Deco 2015). As a high order motor area, Broca's area may be well set up to produce temporal sequences (Rolls, Deco, et al. 2022b).

This connectivity is also consistent with evidence that the inferior parietal cortex is involved in language-based semantic processing and phonological operations (Coslett and Schwartz 2018). In this context, it has been suggested that the parietal cortex is involved in the transcoding of sound-based representations into a format that can drive action systems (Coslett and Schwartz 2018).

Conclusions and overview

Intraparietal areas LIP, VIP, MIP, and AIP have connectivity from early cortical visual areas, and to visuomotor areas such as the frontal eye fields, consistent with functions in the control of eye movements including saccades and tracking.

Five superior parietal area 7 regions receive from similar areas and from the intraparietal areas, but also receive somatosensory inputs and project to premotor areas including area 6, consistent with functions in performing actions to reach for, grasp, and manipulate objects.

In the inferior anterior parietal cortex, PFop and PFt are mainly somatosensory, and PFcm receives vestibular inputs. PF is mainly somatosensory/premotor, but it also receives visuo-motor input from 7Am, AIP, LIPd and IP2, visual shape information from the posterior inferior temporal visual cortex, reward/punishment information from the orbitofrontal cortex and anterior cingulate cortex, and has additional outputs to the PSL area. PF may be involved in building multimodal shape representations using tactile input, and body image representations, to the semantic level. An implication is that PF may be useful for visually recognizing tactile stimuli and objects, and providing for visuo-motor processing of tactile inputs, and so become important in tool use. PF can be considered as the top of the somatosensory hierarchy.

In the inferior parietal cortex more posteriorly, there is connectivity mainly with visual cortical regions. PFm combines high level visual and auditory object representations with visuo-motor input, reward/punishment input, and frontal pole area 10 sequencing/planning input, and connects to the visuo-motor parts of the posterior cingulate cortex, and thereby introduces visuo-spatial input into the hippocampal system. PGs receives visuo-spatial input from area 7Pm, intraparietal, and inferior temporal visual cortex, and projects to the hippocampal system and posterior cingulate memory-related regions, and thus provides visuo-spatial input for the hippocampal system involved in memory and navigation. PGi receives from object (visual inferior temporal TE and visual–auditory STS regions), the temporal pole, the frontal pole, PGs, and the lateral orbitofrontal cortex, and connects to the posterior part of the posterior cingulate cortex implicated in memory, which in turn connects to the hippocampal system. PGi thus provides a route for object and reward information to reach the hippocampal memory system. PGi also projects to the STS regions with neurons that respond to moving objects and face gesture, and as it receives from PGs, and together with PFm, provides a route for intraparietal and superior parietal motion-related visual information to reach the STS regions where it is important in social interactions. Another possible route for visual motion information to reach the STS regions to be combined with object information is from area 7 regions that have effective connectivity directed to the temporo-parietal-occipital junction area (TPOJ2–3), which in turn has connectivity with STS regions. PGp has connectivity with intraparietal regions involved in coordinate transforms and it is proposed here is involved in idiothetic update of hippocampal visual spatial view representations (Robertson et al. 1998) by its connectivity to the parahippocampal scene (or place) area in ventromedial visual VMV1–3 and medial parahippocampal PHA1–3 (Fig. 7c).

Acknowledgements

Supplementary material

Funding

Ethical permissions

Data and code availability

References

Aguirre GK, D'Esposito M. Topographical disorientation: a synthesis and taxonomy. *Brain*. 1999:122(Pt 9):1613–1628.

Alexander AS, Nitz DA. Retrosplenial cortex maps the conjunction of internal and external spaces. *Nat Neurosci*. 2015:18:1143–1151.

Andersen RA. Encoding of intention and spatial location in the posterior parietal cortex. *Cereb Cortex*. 1995:5:457–469.

Andersen RA, Cui H. Intention, action planning, and decision making in parietal-frontal circuits. *Neuron*. 2009:63:568–583.

Andrews-Hanna JR, Smallwood J, Spreng RN. The default network and self-generated thought: component processes, dynamic control, and clinical relevance. *Ann N Y Acad Sci*. 2014:1316:29–52.

Avila E, Lakshminarasimhan KJ, DeAngelis GC, Angelaki DE. Visual and vestibular selectivity for self-motion in macaque posterior parietal area 7a. *Cereb Cortex*. 2019:29:3932–3947.

Bajaj S, Adhikari BM, Friston KJ, Dhamala M. Bridging the gap: dynamic causal Modeling and granger causality analysis of resting state functional magnetic resonance imaging. *Brain Connect*. 2016:6:652–661.

Baker CM, Burks JD, Briggs RG, Conner AK, Glenn CA, Taylor KN, Sali G, McCoy TM, Battiste JD, O'Donoghue DL, et al. A connectomic atlas of the human cerebrum-chapter 7: the lateral parietal lobe. *Oper Neurosurg (Hagerstown)*. 2018:15:S295–S349.

Bakola S, Gamberini M, Passarelli L, Fattori P, Galletti C. Cortical connections of parietal field PEc in the macaque: linking vision and somatic sensation for the control of limb action. *Cereb Cortex*. 2010:20:2592–2604.

Baldassano C, Esteva A, Fei-Fei L, Beck DM. Two distinct scene-processing networks connecting vision and memory. *eNeuro*. 2016:3:e0178–e0116.

Barton JJ. Disorders of higher visual processing. *Handb Clin Neurol*. 2011:102:223–261.

Baumann O, Mattingley JB. Extrahippocampal contributions to spatial navigation in humans: a review of the neuroimaging evidence. *Hippocampus*. 2021:31:640–657.

Berlucchi G, Vallar G. The history of the neurophysiology and neurology of the parietal lobe. *Handb Clin Neurol*. 2018:151:3–30.

Berti A, Neppi-Modona M. Agnosia (including prosopagnosia and Anosognosia). In: Ramachandran VS, editors. *Encyclopedia of human behavior*. 2nd ed. New York: Academic Press; 2012. pp. 60–67

Berti A, Garbarini F, Neppi-Modona M. Disorders of higher cortical function. In: Zigmond MJ, Rowland LP, Coyle JT, editors. *Neurobiology of brain disorders*. New York: Academic Press; 2015. pp. 525–541.

Boccia M, Sulpizio V, Nemmi F, Guariglia C, Galati G. Direct and indirect parieto-medial temporal pathways for spatial navigation in humans: evidence from resting-state functional connectivity. *Brain Struct Funct*. 2017:222:1945–1957.

Bohbot VD, Corkin S. Posterior parahippocampal place learning in H.M. *Hippocampus*. 2007:17:863–872.

Bonner MF, Price AR. Where is the anterior temporal lobe and what does it do? *J Neurosci*. 2013:33:4213–4215.

Buckner RL, DiNicola LM. The brain's default network: updated anatomy, physiology and evolving insights. *Nat Rev Neurosci*. 2019:20:593–608.

Buckner RL, Andrews-Hanna JR, Schacter DL. The brain's default network: anatomy, function, and relevance to disease. *Ann N Y Acad Sci*. 2008:1124:1–38.

Burgess N, Maguire EA, Spiers HJ, O'Keefe J. A temporoparietal and prefrontal network for retrieving the spatial context of lifelike events. *NeuroImage*. 2001:14:439–453.

Byrne P, Becker S, Burgess N. Remembering the past and imagining the future: a neural model of spatial memory and imagery. *Psychol Rev*. 2007:114:340–375.

Caspers S, Zilles K. Microarchitecture and connectivity of the parietal lobe. *Handb Clin Neurol*. 2018:151:53–72.

Caspers S, Eickhoff SB, Geyer S, Scheperjans F, Mohlberg H, Zilles K, Amunts K. The human inferior parietal lobule in stereotaxic space. *Brain Struct Funct*. 2008:212:481–495.

Cavada C, Goldman-Rakic PS. Posterior parietal cortex in rhesus monkey: II. Evidence for segregated corticocortical networks linking sensory and limbic areas with the frontal lobe. *J Comp Neurol*. 1989a:287:422–445.

Cavada C, Goldman-Rakic PS. Posterior parietal cortex in rhesus monkey: I. Parcellation of areas based on distinctive limbic and sensory corticocortical connections. *J Comp Neurol*. 1989b:287: 393–421.

Cavanna AE, Trimble MR. The precuneus: a review of its functional anatomy and behavioural correlates. *Brain*. 2006:129: 564–583.

Chen A, Gu Y, Liu S, DeAngelis GC, Angelaki DE. Evidence for a causal contribution of macaque vestibular, but not intraparietal, cortex to heading perception. *J Neurosci*. 2016a:36:3789–3798.

Chen M, Li B, Guang J, Wei L, Wu S, Liu Y, Zhang M. Two subdivisions of macaque LIP process visual-oculomotor information differently. *Proc Natl Acad Sci U S A*. 2016b:113:E6263–E6270.

Clark IA, Maguire EA. Remembering preservation in hippocampal amnesia. *Annu Rev Psychol*. 2016:67:51–82.

Colby CL, Duhamel JR, Goldberg ME. Ventral intraparietal area of the macaque: anatomic location and visual response properties. *J Neurophysiol*. 1993:69:902–914.

Colby CL, Duhamel JR, Goldberg ME. Visual, presaccadic, and cognitive activation of single neurons in monkey lateral intraparietal area. *J Neurophysiol*. 1996:76:2841–2852.

Colclough GL, Smith SM, Nichols TE, Winkler AM, Sotiropoulos SN, Glasser MF, Van Essen DC, Woolrich MW. The heritability of multi-modal connectivity in human brain activity. *elife*. 2017:6:e20178.

Coslett HB, Schwartz MF. The parietal lobe and language. *Handb Clin Neurol*. 2018:151:365–375.

Craig AD. Significance of the insula for the evolution of human awareness of feelings from the body. *Ann N Y Acad Sci*. 2011:1225: 72–82.

Critchley M. *The parietal lobes*. London: Arnold; 1953

Davis SW, Wing EA, Cabeza R. Contributions of the ventral parietal cortex to declarative memory. *Handb Clin Neurol*. 2018:151: 525–553.

Dean HL, Platt ML. Allocentric spatial referencing of neuronal activity in macaque posterior cingulate cortex. *J Neurosci*. 2006:26: 1117–1127.

Deco G, Rolls ET. Neurodynamics of biased competition and co-operation for attention: a model with spiking neurons. *J Neurophysiol*. 2005a:94:295–313.

Deco G, Rolls ET. Attention, short-term memory, and action selection: a unifying theory. *Prog Neurobiol*. 2005b:76:236–256.

Deco G, Cabral J, Woolrich MW, Stevner ABA, van Hartevelt TJ, Kringelbach ML. Single or multiple frequency generators in on-going brain activity: a mechanistic whole-brain model of empirical MEG data. *NeuroImage*. 2017a:152:538–550.

Deco G, Kringelbach ML, Jirsa VK, Ritter P. The dynamics of resting fluctuations in the brain: metastability and its dynamical cortical core. *Sci Rep*. 2017b:7:3095.

Deco G, Cruzat J, Cabral J, Tagliazucchi E, Laufs H, Logothetis NK, Kringelbach ML. Awakening: predicting external stimulation to force transitions between different brain states. *Proc Natl Acad Sci*. 2019:116:18088–18097.

Dere E, Easton A, Nadel L, Huston JP, editors. *Handbook of episodic memory*. Amsterdam: Elsevier; 2008

Dhollander T, Raffelt D, Connelly A. 2016. Unsupervised 3-tissue response function estimation from single-shell or multi-shell diffusion MR data without a co-registered T1 image. *ISMRM Workshop on Breaking the Barriers of Diffusion MRI* 5.

Di Marco S, Fattori P, Galati G, Galletti C, Lappe M, Maltempo T, Serra C, Sulpizio V, Pitzalis S. Preference for locomotion-compatible curved paths and forward direction of self-motion in somatomotor and visual areas. *Cortex*. 2021:137: 74–92.

DiNicola LM, Braga RM, Buckner RL. Parallel distributed networks dissociate episodic and social functions within the individual. *J Neurophysiol*. 2020:123:1144–1179.

Ekstrom AD, Ranganath C. Space, time, and episodic memory: the hippocampus is all over the cognitive map. *Hippocampus*. 2018:28: 680–687.

Ekstrom AD, Arnold AE, Iaria G. A critical review of the allocentric spatial representation and its neural underpinnings: toward a network-based perspective. *Front Hum Neurosci*. 2014:8: 803.

Elman JA, Rosner ZA, Cohn-Sheehy BI, Cerreta AG, Shimamura AP. Dynamic changes in parietal activation during encoding: implications for human learning and memory. *NeuroImage*. 2013:82: 44–52.

Epstein R. The cortical basis of visual scene processing. *Vis Cogn*. 2005:12:954–978.

Epstein RA. Parahippocampal and retrosplenial contributions to human spatial navigation. *Trends Cogn Sci*. 2008:12:388–396.

Epstein RA, Baker CI. Scene perception in the human brain. *Annu Rev Vis Sci*. 2019:5:373–397.

Epstein RA, Julian JB. Scene areas in humans and macaques. *Neuron*. 2013:79:615–617.

Epstein R, Kanwisher N. A cortical representation of the local visual environment. *Nature*. 1998:392:598–601.

Fattori P, Breveglieri R, Bosco A, Gamberini M, Galletti C. Vision for prehension in the medial parietal cortex. *Cereb Cortex*. 2017:27: 1149–1163.

Foster C, Sheng WA, Heed T, Ben HS. The macaque ventral intraparietal area has expanded into three homologue human parietal areas. *Prog Neurobiol*. 2022:209:102185.

Frassle S, Lomakina EI, Razi A, Friston KJ, Buhmann JM, Stephan KE. Regression DCM for fMRI. *NeuroImage*. 2017:155: 406–421.

Freton M, Lemogne C, Bergouignan L, Delaveau P, Lehericy S, Fossati P. The eye of the self: precuneus volume and visual perspective during autobiographical memory retrieval. *Brain Struct Funct*. 2014:219:959–968.

Freyer F, Roberts JA, Becker R, Robinson PA, Ritter P, Breakspear M. Biophysical mechanisms of multistability in resting-state cortical rhythms. *J Neurosci*. 2011:31:6353–6361.

Freyer F, Roberts JA, Ritter P, Breakspear M. A canonical model of multistability and scale-invariance in biological systems. *PLoS Comput Biol*. 2012:8:e1002634.

Friston K. Causal modelling and brain connectivity in functional magnetic resonance imaging. *PLoS Biol*. 2009:7:e33.

Funahashi S, Bruce CJ, Goldman-Rakic PS. Mnemonic coding of visual space in monkey dorsolateral prefrontal cortex. *J Neurophysiol*. 1989:61:331–349.

Galletti C, Fattori P. The dorsal visual stream revisited: stable circuits or dynamic pathways? *Cortex*. 2018:98:203–217.

Galletti C, Battaglini PP, Fattori P. Parietal neurons encoding spatial locations in craniotopic coordinates. *Exp Brain Res*. 1993:96: 221–229.

Gamberini M, Dal Bo G, Breveglieri R, Briganti S, Passarelli L, Fattori P, Galletti C. Sensory properties of the caudal aspect of the macaque's superior parietal lobule. *Brain Struct Funct*. 2018:223: 1863–1879.

Gamberini M, Passarelli L, Fattori P, Galletti C. Structural connectivity and functional properties of the macaque superior parietal lobule. *Brain Struct Funct*. 2020:225:1349–1367.

Gamberini M, Passarelli L, Filippini M, Fattori P, Galletti C. Vision for action: thalamic and cortical inputs to the macaque superior parietal lobule. *Brain Struct Funct*. 2021:226:2951–2966.

Georges-François P, Rolls ET, Robertson RG. Spatial view cells in the primate hippocampus: allocentric view not head direction or eye position or place. *Cereb Cortex*. 1999:9:197–212.

Giarrocco F, Averbeck BB. Organization of parietoprefrontal and temporoprefrontal networks in the macaque. *J Neurophysiol*. 2021:126: 1289–1309.

Gilbert SJ, Burgess PW. Executive function. *Curr Biol*. 2008:18: R110–R114.

Gilson M, Moreno-Bote R, Ponce-Alvarez A, Ritter P, Deco G. Estimation of directed effective connectivity from fMRI functional connectivity hints at asymmetries in the cortical connectome. *PLoS Comput Biol*. 2016:12:e1004762.

Glasser MF, Sotiropoulos SN, Wilson JA, Coalson TS, Fischl B, Andersson JL, Xu J, Jbabdi S, Webster M, Polimeni JR, et al. The minimal preprocessing pipelines for the human connectome project. *NeuroImage*. 2013:80:105–124.

Glasser MF, Coalson TS, Robinson EC, Hacker CD, Harwell J, Yacoub E, Ugurbil K, Andersson J, Beckmann CF, Jenkinson M, et al. A multimodal parcellation of human cerebral cortex. *Nature*. 2016a:536: 171–178.

Glasser MF, Smith SM, Marcus DS, Andersson JL, Auerbach EJ, Behrens TE, Coalson TS, Harms MP, Jenkinson M, Moeller S, et al. The human connectome Project's neuroimaging approach. *Nat Neurosci*. 2016b:19:1175–1187.

Gnadt JW, Andersen RA. Memory related motor planning activity in posterior parietal cortex of macaque. *Exp Brain Res*. 1988:70: 216–220.

Goldman-Rakic PS. The prefrontal landscape: implications of functional architecture for understanding human mentation and the central executive. *Philos Trans R Soc B*. 1996:351:1445–1453.

Grabenhorst F, Rolls ET. Value, pleasure, and choice in the ventral prefrontal cortex. *Trends Cogn Sci*. 2011:15:56–67.

Griffanti L, Salimi-Khorshidi G, Beckmann CF, Auerbach EJ, Douaud G, Sexton CE, Zsoldos E, Ebmeier KP, Filippini N, Mackay CE, et al. ICA-based artefact removal and accelerated fMRI acquisition for improved resting state network imaging. *NeuroImage*. 2014:95: 232–247.

Grusser OJ, Pause M, Schreiter U. Localization and responses of neurones in the parieto-insular vestibular cortex of awake monkeys (*Macaca fascicularis*). *J Physiol*. 1990:430:537–557.

Habib M, Sirigu A. Pure topographical disorientation: a definition and anatomical basis. *Cortex*. 1987:23:73–85.

Hassabis D, Kumaran D, Maguire EA. Using imagination to understand the neural basis of episodic memory. *J Neurosci*. 2007:27: 14365–14374.

Hasselmo ME, Rolls ET, Baylis GC. The role of expression and identity in the face-selective responses of neurons in the temporal visual cortex of the monkey. *Behav Brain Res*. 1989a:32:203–218.

Hasselmo ME, Rolls ET, Baylis GC, Nalwa V. Object-centred encoding by face-selective neurons in the cortex in the superior temporal sulcus of the monkey. *Exp Brain Res*. 1989b:75: 417–429.

Huang RS, Sereno MI. Multisensory and sensorimotor maps. *Handb Clin Neurol*. 2018:151:141–161.

Huang C-C, Rolls ET, Hsu C-CH, Feng J, Lin C-P. Extensive cortical connectivity of the human hippocampal memory system: beyond the "what" and "where" dual-stream model. *Cereb Cortex*. 2021:31: 4652–4669.

Huang CC, Rolls ET, Feng J, Lin CP. An extended human connectome project multimodal parcellation atlas of the human cortex and subcortical areas. *Brain Struct Funct*. 2022:227:763–778.

Huber J, Ruehl M, Flanagin V, Zu EP. Delineating neural responses and functional connectivity changes during vestibular and nociceptive stimulation reveal the uniqueness of cortical vestibular processing. *Brain Struct Funct*. 2022:227:779–791.

Jeurissen B, Tournier JD, Dhollander T, Connelly A, Sijbers J. Multi-tissue constrained spherical deconvolution for improved analysis of multi-shell diffusion MRI data. *NeuroImage*. 2014:103: 411–426.

Jones EG, Powell TPS. An anatomical study of converging sensory pathways within the cerebral cortex of the monkey. *Brain*. 1970:93: 793–820.

Kamps FS, Julian JB, Kubilius J, Kanwisher N, Dilks DD. The occipital place area represents the local elements of scenes. *NeuroImage*. 2016:132:417–424.

Kim JG, Aminoff EM, Kastner S, Behrmann M. A neural basis for developmental topographic disorientation. *J Neurosci*. 2015:35: 12954–12969.

Klingner CM, Witte OW. Somatosensory deficits. *Handb Clin Neurol*. 2018:151:185–206.

Kolb B, Whishaw IQ. *Fundamentals of human neuropsychology*. New York: Worth; 2015

Kolster H, Peeters R, Orban GA. The retinotopic organization of the human middle temporal area MT/V5 and its cortical neighbors. *J Neurosci*. 2010:30:9801–9820.

Kravitz DJ, Saleem KS, Baker CI, Mishkin M. A new neural framework for visuospatial processing. *Nat Rev Neurosci*. 2011:12: 217–230.

Kringelbach ML, Deco G. Brain states and transitions: insights from computational neuroscience. *Cell Rep*. 2020:32: 108128.

Kringelbach ML, McIntosh AR, Ritter P, Jirsa VK, Deco G. The rediscovery of slowness: exploring the timing of cognition. *Trends Cogn Sci*. 2015:19:616–628.

Kropff E, Carmichael JE, Moser MB, Moser EI. Speed cells in the medial entorhinal cortex. *Nature*. 2015:523:419–424.

Kuznetsov YA. *Elements of applied bifurcation theory*. New York: Springer Science & Business Media; 2013

Lasne G, Piazza M, Dehaene S, Kleinschmidt A, Eger E. Discriminability of numerosity-evoked fMRI activity patterns in human intra-parietal cortex reflects behavioral numerical acuity. *Cortex*. 2019:114:90–101.

Liu B, Tian Q, Gu Y. Robust vestibular self-motion signals in macaque posterior cingulate region. *elife*. 2021:10:e64569.

Ma Q, Rolls ET, Huang C-C, Cheng W, Feng J. Extensive cortical functional connectivity of the human hippocampal memory system. *Cortex*. 2022:147:83–101.

Maguire EA. The retrosplenial contribution to human navigation: a review of lesion and neuroimaging findings. *Scand J Psychol*. 2001:42:225–238.

Maguire EA, Intraub H, Mullally SL. Scenes, spaces, and memory traces: what does the hippocampus do? *Neuroscientist*. 2016:22: 432–439.

Maltempo T, Pitzalis S, Bellagamba M, Di Marco S, Fattori P, Galati G, Galletti C, Sulpizio V. Lower visual field preference for the visuomotor control of limb movements in the human dorsomedial parietal cortex. *Brain Struct Funct*. 2021:226:2989–3005.

Margulies DS, Vincent JL, Kelly C, Lohmann G, Uddin LQ, Biswal BB, Villringer A, Castellanos FX, Milham MP, Petrides M. Precuneus shares intrinsic functional architecture in humans and monkeys. *Proc Natl Acad Sci U S A*. 2009:106:20069–20074.

Markov NT, Vezoli J, Chameau P, Falchier A, Quilodran R, Huissoud C, Lamy C, Misery P, Giroud P, Ullman S, et al. Anatomy of hierarchy: feedforward and feedback pathways in macaque visual cortex. *J Comp Neurol*. 2014:522:225–259.

McCabe C, Rolls ET, Bilderbeck A, McGlone F. Cognitive influences on the affective representation of touch and the sight of touch in the human brain. *Soc Cogn Affect Neurosci*. 2008:3:97–108.

Miller JF, Neufang M, Solway A, Brandt A, Trippel M, Mader I, Hefft S, Merkow M, Polyn SM, Jacobs J, et al. Neural activity in human hippocampal formation reveals the spatial context of retrieved memories. *Science*. 2013:342:1111–1114.

Montaldi D, Spencer TJ, Roberts N, Mayes AR. The neural system that mediates familiarity memory. *Hippocampus*. 2006:16:504–520.

Morris R, Petrides M, Pandya DN. Architecture and connections of retrosplenial area 30 in the rhesus monkey (*Macaca mulatta*). *Eur J Neurosci*. 1999:11:2506–2518.

Mountcastle VB, Lynch JC, Georgopoulos A, Sakata H, Acuna C. Posterior parietal association cortex of the monkey: command functions for operations within extrapersonal space. *J Neurophysiol*. 1975:38:871–908.

Munuera J, Duhamel JR. The role of the posterior parietal cortex in saccadic error processing. *Brain Struct Funct*. 2020:225:763–784.

Natu VS, Arcaro MJ, Barnett MA, Gomez J, Livingstone M, Grill-Spector K, Weiner KS. Sulcal depth in the medial ventral temporal cortex predicts the location of a place-selective region in macaques, children, and adults. *Cereb Cortex*. 2021:31:48–61.

Neal JW, Pearson RC, Powell TP. The connections of area PG, 7a, with cortex in the parietal, occipital and temporal lobes of the monkey. *Brain Res*. 1990:532:249–264.

O'Mara SM, Rolls ET, Berthoz A, Kesner RP. Neurons responding to whole-body motion in the primate hippocampus. *J Neurosci*. 1994:14:6511–6523.

Orban GA, Sepe A, Bonini L. Parietal maps of visual signals for bodily action planning. *Brain Struct Funct*. 2021:226:2967–2988.

Papagno C. Memory deficits. In: *Handbook of clinical neurology*. Vol. 151. Oxford: Parietal Cortex; 2018. pp. 377–393

Passarelli L, Gamberini M, Fattori P. The superior parietal lobule of primates: a sensory-motor hub for interaction with the environment. *J Integr Neurosci*. 2021:20:157–171.

Passingham RE. *Understanding the prefrontal cortex: selective advantage, connectivity and neural operations*. Oxford: Oxford University Press; 2021

Patel GH, Sestieri C, Corbetta M. The evolution of the temporoparietal junction and posterior superior temporal sulcus. *Cortex*. 2019:118:38–50.

Perrett DI, Rolls ET, Caan W. Visual neurons responsive to faces in the monkey temporal cortex. *Exp Brain Res*. 1982:47:329–342.

Perrett D, Mistlin A, Chitty A. Visual neurons responsive to faces. *Trends Neurosci*. 1987:10:358–364.

Persichetti AS, Dilks DD. Distinct representations of spatial and categorical relationships across human scene-selective cortex. *Proc Natl Acad Sci U S A*. 2019:116:21312–21317.

Pitzalis S, Sereno MI, Committeri G, Fattori P, Galati G, Tosoni A, Galletti C. The human homologue of macaque area V6A. *NeuroImage*. 2013:82:517–530.

Pitzalis S, Fattori P, Galletti C. The human cortical areas V6 and V6A. *Vis Neurosci*. 2015:32:E007.

Pitzalis S, Serra C, Sulpizio V, Di Marco S, Fattori P, Galati G, Galletti C. A putative human homologue of the macaque area PEc. *NeuroImage*. 2019:202:116092.

Platt ML, Glimcher PW. Neural correlates of decision variables in parietal cortex. *Nature*. 1999:400:233–238.

Power JD, Cohen AL, Nelson SM, Wig GS, Barnes KA, Church JA, Vogel AC, Laumann TO, Miezin FM, Schlaggar BL, et al. Functional network organization of the human brain. *Neuron*. 2011:72:665–678.

Price AR, Bonner MF, Peelle JE, Grossman M. Converging evidence for the neuroanatomic basis of combinatorial semantics in the angular gyrus. *J Neurosci*. 2015:35:3276–3284.

Quesque F, Brass M. The role of the temporoparietal junction in self-other distinction. *Brain Topogr*. 2019:32:943–955.

Raffi M, Maioli MG, Squatrito S. Optic flow direction coding in area PEc of the behaving monkey. *Neuroscience*. 2011:194:136–149.

Raichle ME, MacLeod AM, Snyder AZ, Powers WJ, Gusnard DA, Shulman GL. A default mode of brain function. *Proc Natl Acad Sci U S A*. 2001:98:676–682.

Razi A, Seghier ML, Zhou Y, McColgan P, Zeidman P, Park HJ, Sporns O, Rees G, Friston KJ. Large-scale DCMs for resting-state fMRI. *Netw Neurosci*. 2017:1:222–241.

Rizzolatti G, Rozzi S. The mirror mechanism in the parietal lobe. *Handb Clin Neurol*. 2018:151:555–573.

Robertson RG, Rolls ET, Georges-François P. Spatial view cells in the primate hippocampus: effects of removal of view details. *J Neurophysiol*. 1998:79:1145–1156.

Rolls ET. Neurons in the cortex of the temporal lobe and in the amygdala of the monkey with responses selective for faces. *Hum Neurobiol*. 1984:3:209–222.

Rolls ET. Functions of the primate temporal lobe cortical visual areas in invariant visual object and face recognition. *Neuron*. 2000:27:205–218.

Rolls ET. The affective and cognitive processing of touch, oral texture, and temperature in the brain. *Neurosci Biobehav Rev*. 2010:34:237–245.

Rolls ET. *Cerebral cortex: principles of operation*. Oxford: Oxford University Press; 2016

Rolls ET. The storage and recall of memories in the hippocampo-cortical system. *Cell Tissue Res*. 2018:373:577–604.

Rolls ET. *The orbitofrontal cortex*. Oxford: Oxford University Press; 2019a

Rolls ET. The cingulate cortex and limbic systems for emotion, action, and memory. *Brain Struct Funct*. 2019b:224:3001–3018.

Rolls ET. The orbitofrontal cortex and emotion in health and disease, including depression. *Neuropsychologia*. 2019c:128:14–43.

Rolls ET. Spatial coordinate transforms linking the allocentric hippocampal and egocentric parietal primate brain systems for memory, action in space, and navigation. *Hippocampus*. 2020:30:332–353.

Rolls ET. Neurons including hippocampal spatial view cells, and navigation in primates including humans. *Hippocampus*. 2021a:31:593–611.

Rolls ET. Learning invariant object and spatial view representations in the brain using slow unsupervised learning. *Front Comput Neurosci*. 2021b:15:686239.

Rolls ET. *Brain computations: what and how*. Oxford: Oxford University Press; 2021c

Rolls ET. Hippocampal spatial view cells for memory and navigation, and their underlying connectivity in humans. *Hippocampus*. 2022a: in revision.

Rolls ET. The hippocampus, ventromedial-prefrontal cortex, and episodic and semantic memory. *Prog Neurobiol*. 2022b: in revision.

Rolls ET, Deco G. Networks for memory, perception, and decision-making, and beyond to how the syntax for language might be implemented in the brain. *Brain Res*. 2015:1621:316–334.

Rolls ET, Treves A. The neuronal encoding of information in the brain. *Prog Neurobiol*. 2011:95:448–490.

Rolls ET, Wirth S. Spatial representations in the primate hippocampus, and their functions in memory and navigation. *Prog Neurobiol*. 2018:171:90–113.

Rolls ET, Perrett D, Thorpe SJ, Puerto A, Roper-Hall A, Maddison S. Responses of neurons in area 7 of the parietal cortex to objects of different significance. *Brain Res*. 1979:169:194–198.

Rolls ET, Robertson RG, Georges-François P. Spatial view cells in the primate hippocampus. *Eur J Neurosci*. 1997a:9:1789–1794.

Rolls ET, Treves A, Tovee MJ. The representational capacity of the distributed encoding of information provided by populations of neurons in the primate temporal visual cortex. *Exp Brain Res*. 1997b:114:177–185.

Rolls ET, Treves A, Tovee MJ, Panzeri S. Information in the neuronal representation of individual stimuli in the primate temporal visual cortex. *J Comput Neurosci*. 1997c:4:309–333.

Rolls ET, Treves A, Robertson RG, Georges-François P, Panzeri S. Information about spatial view in an ensemble of primate hippocampal cells. *J Neurophysiol*. 1998:79:1797–1813.

Rolls ET, O'Doherty J, Kringelbach ML, Francis S, Bowtell R, McGlone F. Representations of pleasant and painful touch in the human orbitofrontal and cingulate cortices. *Cereb Cortex*. 2003:13: 308–317.

Rolls ET, Tromans J, Stringer SM. Spatial scene representations formed by self-organizing learning in a hippocampal extension of the ventral visual system. *Eur J Neurosci*. 2008:28:2116–2127.

Rolls ET, Kellerhals MB, Nichols TE. Age differences in the brain mechanisms of good taste. *NeuroImage*. 2015:113:298–309.

Rolls ET, Wirth S, Deco G, Huang C-C, Feng J. The human posterior cingulate, retrosplenial and medial parietal cortex effective connectome, and implications for memory and navigation. *Hum Brain Mapp*. 2022, in review.

Rolls ET, Deco G, Huang C-C, Feng J. Multiple cortical visual streams in humans. *Cereb Cortex*. 2022a. https://doi.org/10.1093/cercor/bhac276

Rolls ET, Deco G, Huang C-C, Feng J. The human language effective connectome. *NeuroImage*. 2022b:258:119352.

Rolls ET, Deco G, Huang CC, Feng J. The human orbitofrontal cortex, vmPFC, and anterior cingulate cortex effective connectome: emotion, memory, and action. *Cereb Cortex*. 2022c.https://doi.org/10.1093/cercor/bhac1070.

Rolls ET, Deco G, Huang CC, Feng J. The effective connectivity of the human hippocampal memory system. *Cereb Cortex*. 2022d. https://doi.org/10.1093/cercor/bhab1442.

Ronchi R, Park HD, Blanke O. Bodily self-consciousness and its disorders. *Handb Clin Neurol*. 2018:151:313–330.

Salimi-Khorshidi G, Douaud G, Beckmann CF, Glasser MF, Griffanti L, Smith SM. Automatic denoising of functional MRI data: combining independent component analysis and hierarchical fusion of classifiers. *NeuroImage*. 2014:90:449–468.

Satterthwaite TD, Elliott MA, Gerraty RT, Ruparel K, Loughead J, Calkins ME, Eickhoff SB, Hakonarson H, Gur RC, Gur RE, et al. An improved framework for confound regression and filtering for control of motion artifact in the preprocessing of resting-state functional connectivity data. *NeuroImage*. 2013:64: 240–256.

Scheirer J, Ray WS, Hare N. The analysis of ranked data derived from completely randomized factorial designs. *Biometrics*. 1976:32: 429–434.

Schurz M, Tholen MG, Perner J, Mars RB, Sallet J. Specifying the brain anatomy underlying temporo-parietal junction activations for theory of mind: a review using probabilistic atlases from different imaging modalities. *Hum Brain Mapp*. 2017:38:4788–4805.

Shallice T, Burgess P. The domain of supervisory processes and temporal organization of behaviour. *Philos Trans R Soc B*. 1996:351: 1405–1411.

Shallice T, Cipolotti L. The prefrontal cortex and neurological impairments of active thought. *Annu Rev Psychol*. 2018:69:157–180.

Silson EH, Steel AD, Baker CI. Scene-selectivity and retinotopy in medial parietal cortex. *Front Hum Neurosci*. 2016:10:412.

Silson EH, Steel A, Kidder A, Gilmore AW, Baker CI. Distinct subdivisions of human medial parietal cortex support recollection of people and places. *elife*. 2019:8:e47391.

Sinha N. 2022. Non-parametric alternative of 2-way ANOVA (ScheirerRayHare) MATLAB central file exchange. https://www.mathworks.com/matlabcentral/fileexchange/96399-non-parametric-alternative-of-96392-way-anova-scheirerrayhare.

Smith SM. Fast robust automated brain extraction. *Hum Brain Mapp*. 2002:17:143–155.

Smith SM, Beckmann CF, Andersson J, Auerbach EJ, Bijsterbosch J, Douaud G, Duff E, Feinberg DA, Griffanti L, Harms MP, et al. Resting-state fMRI in the human connectome project. *NeuroImage*. 2013:80:144–168.

Smith RE, Tournier JD, Calamante F, Connelly A. SIFT2: enabling dense quantitative assessment of brain white matter connectivity using streamlines tractography. *NeuroImage*. 2015:119: 338–351.

Snyder LH, Grieve KL, Brotchie P, Andersen RA. Separate body- and world-referenced representations of visual space in parietal cortex. *Nature*. 1998:394:887–891.

Spiers HJ, Maguire EA. Thoughts, behaviour, and brain dynamics during navigation in the real world. *NeuroImage*. 2006:31:1826–1840.

Stringer SM, Rolls ET, Trappenberg TP. Self-organizing continuous attractor network models of hippocampal spatial view cells. *Neurobiol Learn Mem*. 2005:83:79–92.

Sulpizio V, Galati G, Fattori P, Galletti C, Pitzalis S. A common neural substrate for processing scenes and egomotion-compatible visual motion. *Brain Struct Funct*. 2020:225:2091–2110.

Szpunar KK, Chan JC, McDermott KB. Contextual processing in episodic future thought. *Cereb Cortex*. 2009:19:1539–1548.

Takahashi N, Kawamura M, Shiota J, Kasahata N, Hirayama K. Pure topographic disorientation due to right retrosplenial lesion. *Neurology*. 1997:49:464–469.

Takashima A, Petersson KM, Rutters F, Tendolkar I, Jensen O, Zwarts MJ, McNaughton BL, Fernandez G. Declarative memory consolidation in humans: a prospective functional magnetic resonance imaging study. *Proc Natl Acad Sci U S A*. 2006:103: 756–761.

Teng E, Squire LR. Memory for places learned long ago is intact after hippocampal damage. *Nature*. 1999:400:675–677.

Tosoni A, Pitzalis S, Committeri G, Fattori P, Galletti C, Galati G. Resting-state connectivity and functional specialization in human medial parieto-occipital cortex. *Brain Struct Funct*. 2015:220:3307–3321.

Tsitsiklis M, Miller J, Qasim SE, Inman CS, Gross RE, Willie JT, Smith EH, Sheth SA, Schevon CA, Sperling MR, et al. Single-neuron representations of spatial targets in humans. *Curr Biol*. 2020:30:245, e244–253.

Uddin LQ, Supekar K, Amin H, Rykhlevskaia E, Nguyen DA, Greicius MD, Menon V. Dissociable connectivity within human angular gyrus and intraparietal sulcus: evidence from functional and structural connectivity. *Cereb Cortex*. 2010:20:2636–2646.

Underwood AG, Guynn MJ, Cohen AL. The future orientation of past memory: the role of BA 10 in prospective and retrospective retrieval modes. *Front Hum Neurosci*. 2015:9:668.

Urgen BA, Orban GA. The unique role of parietal cortex in action observation: functional organization for communicative and manipulative actions. *NeuroImage*. 2021:237:118220.

Valdes-Sosa PA, Roebroeck A, Daunizeau J, Friston K. Effective connectivity: influence, causality and biophysical modeling. *NeuroImage*. 2011:58:339–361.

Vallar G, Calzolari E. Unilateral spatial neglect after posterior parietal damage. *Handb Clin Neurol*. 2018:151:287–312.

van Assche M, Kebets V, Vuilleumier P, Assal F. Functional dissociations within posterior parietal cortex during scene integration and viewpoint changes. *Cereb Cortex*. 2016:26:586–598.

Van Essen DC, Glasser MF. Parcellating cerebral cortex: how invasive animal studies inform noninvasive mapmaking in humans. *Neuron*. 2018:99:640–663.

Van Essen DC, Smith SM, Barch DM, Behrens TE, Yacoub E, Ugurbil K, WU-MH C. The WU-Minn human connectome project: an overview. *NeuroImage*. 2013:80:62–79.

Vann SD, Aggleton JP, Maguire EA. What does the retrosplenial cortex do? *Nat Rev Neurosci*. 2009:10:792–802.

Vedder LC, Miller AMP, Harrison MB, Smith DM. Retrosplenial cortical neurons encode navigational cues, trajectories and reward locations during goal directed navigation. *Cereb Cortex*. 2017:27: 3713–3723.

Verhagen JV, Kadohisa M, Rolls ET. The primate insular/opercular taste cortex: neuronal representations of the viscosity, fat texture, grittiness, temperature and taste of foods. *J Neurophysiol*. 2004:92:1685–1699.

Wirth S, Baraduc P, Plante A, Pinede S, Duhamel JR. Gaze-informed, task-situated representation of space in primate hippocampus during virtual navigation. *PLoS Biol*. 2017:15: e2001045.

Yokoyama C, Autio JA, Ikeda T, Sallet J, Mars RB, Van Essen DC, Glasser MF, Sadato N, Hayashi T. Comparative connectomics of the primate social brain. *NeuroImage*. 2021:245: 118693.